

**High Performance
Photon Counting**

User Handbook

**Leica MP-FLIM
and D-FLIM**

Fluorescence Lifetime

Microscopy Systems

Based on bh TCSPC Technique



Becker & Hickl GmbH



Becker & Hickl GmbH
Nahmitzer Damm 30
12277 Berlin
Germany
Tel. +49 / 30 / 787 56 32
FAX +49 / 30 / 787 57 34
<http://www.becker-hickl.com>
email: info@becker-hickl.com

Leica Microsystems Heidelberg GmbH
Am Friedensplatz 3
D-68165 Mannheim
Tel. +49 621 7028 0
Fax +49 621 7028 1180
email: llt.support@leica-microsystems.com
<http://www.confocal-microscopy.com>

1st Edition, May 2006

This handbook is subject to copyright. However, reproduction of small portions of the material in scientific papers or other non-commercial publications is considered fair use under the copyright law. It is requested that a complete citation be included in the publication. If you require confirmation please feel free to contact Leica Microsystems or Becker & Hickl.

Contents

Introduction.....	1
Why Use FLIM.....	1
Requirements to a FLIM Technique.....	4
Multi-Dimensional Time-Correlated Single Photon Counting.....	5
One-Photon FLIM versus Multi-Photon FLIM.....	8
The Leica FLIM Systems.....	11
System Configuration.....	11
SP2 Setup for FLIM measurement.....	12
Laser Setup for D FLIM.....	12
Laser Setup for MP FLIM.....	13
Setup of Imaging Parameters in LCS Software.....	14
Scanning a Sample.....	16
FLIM Data Acquisition Software.....	18
DCC-100 Software.....	18
SPCM Software.....	19
TCSPC System Parameters.....	20
Measurement Control Parameters.....	21
CFD, SYNC and TAC Parameters.....	22
Data Format and Page Control.....	22
Scan Parameters.....	23
Access of System Parameters from Main Panel.....	23
Display of Images in the SPCM Software.....	24
Online Display.....	24
Display Parameters.....	24
Window Parameters.....	25
Saving Setup and Measurement Data.....	27
Loading Setup and Measurement Data.....	28
Setup Files Delivered with the FLIM System.....	29
Predefined Setups.....	30
FLIM Measurements.....	31
Steps of a FLIM Measurement.....	31
Details of FLIM Data Acquisition.....	33
Count Rates.....	33
Photobleaching.....	34
Acquisition Time of FLIM.....	34
Image Size.....	36
Data Analysis.....	37
Introduction.....	37
Analysing fluorescence lifetime images.....	39
Loading of FLIM Data.....	39
Hot Spot and Region of Interest Selection.....	40
Instrument Response Function.....	41
Fit Selection Parameters.....	41
Binning of Pixels in the Data Analysis.....	42
Model Selection.....	44
Calculation of the Lifetime Image.....	46
Display of Lifetime Images.....	47
Lifetime Parameter Histogram.....	48
Special Commands.....	48
Special FLIM System Configurations.....	50
Detectors for Multiphoton Direct Detection FLIM.....	50
Multiphoton Multi-Wavelength FLIM.....	51
Detectors for Confocal FLIM.....	51

Dual-Detector Systems	52
Applications	53
Measurement of Local Environment Parameters.....	53
Fluorescence Resonance Energy Transfer (FRET)	53
Autofluorescence Microscopy of Tissue	56
References.....	57
Index	63

Introduction

The Leica D FLIM and MP FLIM systems are add-ons of the TCS SP2 and TCS SP5 laser scanning microscopes. The systems are based on the multi-dimensional TCSPC technique [18] and the SPC-830 TCSPC modules of Becker & Hickl. This handbook should be considered a supplement to the handbooks of the Leica TCS SP2, Leica TCS SP5, and the bh TCSPC Handbook [19]. Moreover, we recommend [18] as supplementary literature.

Why Use FLIM

Since their broad introduction in the early 90s confocal and two-photon laser scanning microscopes have initiated a breakthrough in biomedical imaging [41, 65, 82, 100]. The applicability of multi-photon excitation, the optical sectioning capability and the superior contrast of these instruments make them an ideal choice for fluorescence imaging of biological samples.

However, the fluorescence of organic molecules is not only characterised by the emission intensity and the emission spectrum, it has also a characteristic lifetime. In the simplest case, the fluorescence lifetime can be used to distinguish between different fluorophores. Moreover, the fluorescence lifetime is not only different for different fluorophores, it also depends on the molecular environment of the fluorophore molecules. Any interaction between an excited molecule and its environment in a predictable way changes the fluorescence lifetime. Since the lifetime does not depend on the concentration of the fluorophore fluorescence lifetime imaging is a direct approach to the mapping of cell parameters like pH, ion concentrations or oxygen saturation, protein interaction, and other effects on the molecular scale.

The Fluorescence Decay Function

When an organic dye is excited by light of appropriate wavelength a part of the light is absorbed. A fraction of the absorbed light is converted into heat; the rest is emitted at a wavelength longer than the excitation wavelength. The effect is known as fluorescence. The fluorescence light not only has a characteristic spectrum it is also emitted with a characteristic time constant, the fluorescence lifetime or fluorescence decay time [73]. The fluorescence lifetime becomes apparent if a sample is excited by light pulses shorter than a few nanoseconds, see Fig. 1.

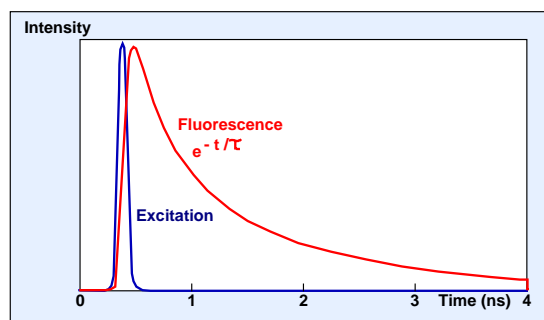


Fig. 1: Decay of the fluorescence (red) after excitation with a short light pulse (blue)

In the simplest case, the fluorescence lifetime can be used as an additional parameter to separate or identify the emission of different fluorophores. The application of the lifetime as a separation parameter is particularly useful to distinguish the autofluorescence components in tissues. These components often have poorly defined fluorescence spectra but can be distinguished by their fluorescence lifetime [69]. FLIM has also been used to verify the laser-based transfection of cells with GFP [97].

Fluorescence Quenching

An excited molecule can also dissipate the absorbed energy by interaction with other molecules. The effect is called fluorescence quenching. The fluorescence lifetime, τ , becomes shorter than the normally observed fluorescence lifetime, τ_0 , see Fig. 2. Typical quenchers are oxygen, halogens, and heavy metal ions, and a variety of organic molecules. The fluorescence lifetime of most fluorophores depends more or less on the concentration of ions in the local environment and on the oxygen concentration. For fluorescence lifetime microscopy it is important that the rate constant of fluorescence quenching depends linearly on the concentration of the quencher. The concentration of the quencher can therefore be directly be obtained from the decrease in the fluorescence lifetime [73].

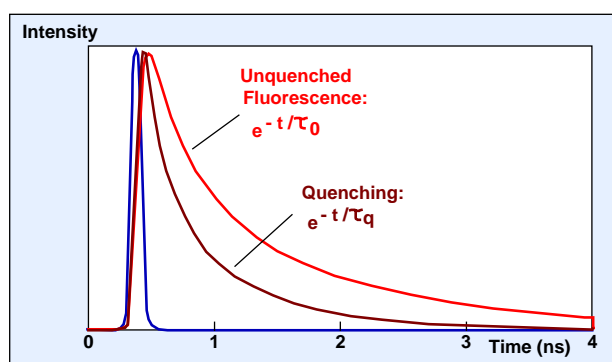


Fig. 2: Fluorescence quenching

Protonation

Many fluorescent molecules have a protonated and a deprotonated form. The equilibrium between both depends on the pH. If the protonated and deprotonated form have different lifetimes the apparent lifetime is an indicator of the pH. A typical representative of the pH-sensitive dyes is 2',7'-bis-(2-carboxyethyl)-5-(and-6)-carboxyfluorescein (BCECF) [54, 57, 73].

Complexes

Many fluorescent molecules, including endogenous fluorophores, form complexes with other molecules, in particular proteins. The fluorescence spectra of these different conformations can be virtually identical, but the fluorescence lifetimes are often different. The exact mechanism of the lifetime changes is not always clear. In practice, it is only important that for almost all dyes the fluorescence lifetime depends more or less on the binding to proteins, DNA or lipids [62, 72, 73, 91, 92, 99]. The lifetime can therefore be used to probe the local environment of dye molecules on the molecular scale, independently of the concentration of the fluorescing molecules.

Extremely strong effects on the decay rates must also be expected if dye molecules are bound to metal surfaces, especially to metallic nano-particles [48, 75].

The fluorescence behaviour of a fluorophore is also influenced by the solvent, especially the solvent polarity [73]. Moreover, when a molecule is in the excited state the solvent molecules around it re-arrange. Consequently, energy is transferred to the solvent, with the result that the emission spectrum is red-shifted. Solvent (or spectral) relaxation in water happens on the time scale of a few ps. However, the relaxation times in viscous solvents and in dye-protein constructs can be of the same order as the fluorescence lifetime. The effects can be measured by TCSPC [86]; applications to cell imaging have not been reported yet.

Aggregation

The radiative and non-radiative decay rates depend also on possible aggregation of the dye molecules. The electron systems of the individual molecules in aggregates are strongly coupled. Therefore the fluorescence behaviour of aggregates differs from that of the single molecules. The lifetime of aggregates can be longer than that of single molecules; on the other hand, the fluorescence may be almost entirely quenched. Aggregation is influenced by the local environment; the associated lifetime changes can be used as a probe function. Aggregation has also been used to observe the internalisation of dyes into cells [61]. However, in most applications aggregation is to be avoided by keeping the dye concentration at a reasonable level.

FRET

A particularly efficient energy transfer process between an excited and a non-excited molecule is fluorescence resonance energy transfer, or FRET. The effect was found by Theodor Förster in 1946 [47]. The effect is also called Förster resonance energy transfer or simply resonance energy transfer (RET). Fluorescence resonance energy transfer is an interaction of two molecules in which the emission band of one molecule overlaps the absorption band of the other. In this case the energy from the first dye, the donor, transfers immediately into the second one, the acceptor. The energy transfer itself does not involve any light emission and absorption. FRET can result in an extremely efficient quenching of the donor fluorescence and consequently in a considerable decrease of the donor lifetime; see Fig. 3.

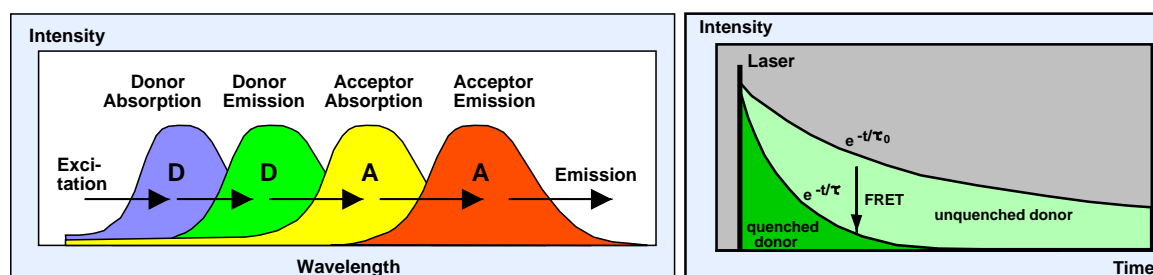


Fig. 3: Fluorescence Resonance Energy Transfer (FRET)

The energy transfer rate from the donor to the acceptor decreases with the sixth power of the distance. Therefore it is noticeable only at distances shorter than 10 nm [73]. FRET is used as a tool to investigate protein-protein interaction. Different proteins are labelled with the donor and the acceptor, and FRET is used as an indicator of the binding state of these proteins. Distances on the nm scale can be determined by measuring the FRET efficiency quantitatively.

Decay Profiles of Biological Samples

It is sometimes believed that FLIM in cells does not require a particularly high time resolution. It is certainly correct that the fluorescence lifetimes of most fluorophores used in cell imaging are on the order of a few ns. However, the lifetime of autofluorescence components and of the quenched donor fraction in FRET experiments can be as short as 100 ps. Lifetimes of dye aggregates in cells have been found as short as 50 ps [61]. The lifetime of fluorophores bound to metallic nano-particles [48, 75] can be 100 ps and shorter.

The fluorophore populations in biological specimens are normally not homogeneous. Several fluorophores may be present in the same pixel, or one fluorophore may exist in different binding or protonation states. The fluorescence decay functions are therefore usually multi-exponential. A few typical decay profiles are shown in Fig. 4.

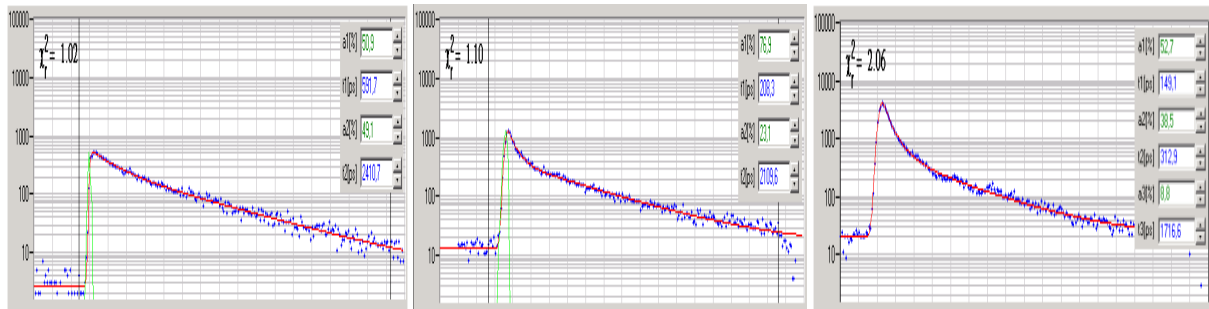


Fig. 4: Decay profiles of biological samples, total length of time axis 10 ns, logarithmic intensity scale. Left to right: CFP-YFP FRET in HEK cell at emission wavelength of CFP, autofluorescence of the stratum corneum of human skin, plant tissue sample

The curves show the fluorescence intensity versus the time in the fluorescence decay. The total length of the time axis is 10 ns; the intensity scale is logarithmic. All curves were measured by TCSPC FLIM. The blue dots are the photon numbers in the subsequent time channels of a selected region of the image; the red curve is a fit by a double-exponential or triple-exponential model. Even without data analysis, it is clearly visible that the decay profiles are not single exponentials.

In the case of CFP YFP FRET the decay profile can be fitted well by a double-exponential model. The fit delivers a lifetime of 590 ps for the interacting donor component, a lifetime of 2.4 ns for the non-interacting donor component, and the respective amplitudes of 51 % and 49 %.

The fluorescence decay of skin autofluorescence is fit by two components of 208 ps and 2.1 ns, with amplitudes of 77 % and 23 %. For the plant tissue even a double-exponential fit is not satisfactory. A triple-exponential fit delivers 150 ps, 313 ps, and 1716 ps, with amplitudes of 53 %, 39 % and 8.8 %, respectively.

There are certainly cases when fitting multi-exponential decay profiles by a single-exponential decay is feasible. These may be pH imaging, oxygen quenching experiments, or ion concentration measurements. Even in FRET experiments a single-exponential fit is acceptable if only the locations of protein interaction in a cell, not the quantitative values are required. In most cases, however, describing the fluorescence of the sample by a single ‘Fluorescence Lifetime’ means discarding useful information.

Requirements to a FLIM Technique

Time Resolution

As shown above the decay profiles of biological samples have components down to 100 ps, possibly even less. Moreover, the decay functions are often multi-exponential. A good FLIM technique should therefore be able to record lifetimes down to less than 100 ps and the components of complex decay profiles.

Efficiency

Under ideal conditions, the lifetime of a single-exponential decay can be obtained from the recorded data with the same accuracy as the intensity [5, 49, 63]. In both cases the standard deviation is \sqrt{N} , with N being the number of photons in the pixels considered. One might therefore conclude that FLIM does not set special requirements to the photon economy. Unfortunately this is not so. An intensity image with a standard deviation of 10% may look pleasing and show the spatial structure of a sample very well. However, lifetime changes investigated by FLIM may be on the order of a few %. Thus, a standard deviation on the order

of 1 % is required. Thus, except for a few relatively trivial cases, FLIM experiments need to record a large number of photons.

An even larger number of photons is required for resolving the components multi-exponential decay functions. Köllner and Wolfrum [63] calculate a number of 400.000 photons for resolving two decay components of 2 ns and 4 ns, with amplitudes of 10% and 90%, respectively. Of course, resolving such decay functions in FLIM images is close to impossible. Fortunately, in practice the lifetimes are wider apart, and the amplitude of the fast component is larger. Such decay profiles can be resolved by analysing some 1000 photons per pixel, see Fig. 4. Nevertheless, a large number of photons must be recorded.

Recording many photons means either a high excitation intensity or a long acquisition time. Therefore photobleaching [42, 80] and photodamage [58, 64, 67] are important issues in precision FLIM experiments. Both effects are more troublesome for FLIM than for intensity imaging because they are likely to change the fluorescence lifetimes [17]. Photobleaching and photodamage are clearly nonlinear for two-photon excitation [80]. A nonlinear component seems to be present also for high intensities of one-photon excitation [25]. A good FLIM technique must therefore not only make best use of the detected photons, it must also be able to work reliably at low intensity.

Multi-Wavelength Detection

In some cases FLIM images are taken in several emission wavelength intervals or under different angle of polarisation [14, 26]. It is important that both recordings be performed simultaneously. This not only reduces the sample exposure and the associated photobleaching, it also avoids the photobleaching of the first recording changing the results of the second one. Only if both recordings are done simultaneously the results are really comparable.

Compatibility with the Scanning Microscope

Laser scanning microscopes with standard scanners scan the sample at pixel dwell times down to a few μs , systems with resonance scanners even faster. Photon rates obtained from typical samples are usually an order of magnitude smaller. It is thus impossible to obtain enough photons for lifetime analysis within a time this short. Consequently, the FLIM system must be able to acquire the photons from a large number of frames run at a pixel rate higher than the photon detection rate.

Another important issue is lateral resolution and depth resolution. Mixing the fluorescence lifetimes of different sample planes or different locations of the sample must be strictly avoided. Thus, the FLIM technique must make full use of the confocal and two-photon excitation features of the microscope [18].

Multi-Dimensional Time-Correlated Single Photon Counting

Time-correlated single photon counting (TCSPC) is an amazingly sensitive technique for recording low-level light signals with picosecond resolution and extremely high precision. TCSPC is based on the detection of single photons of a periodic light signal, the measurement of the detection times, and the reconstruction of the waveform from the individual time measurements. The technique in its classic form is successfully used since the early 70s [79, 101].

Due to the low intensity and low repetition rate of the light sources and the limited speed of the electronics of the 70s and 80s the acquisition times of classic TCSPC applications were extremely long. More important, classic TCSPC was intrinsically one-dimensional, i.e. limited to the recording of the waveform of a periodic light signal. For many years TCSPC was therefore used primarily to record fluorescence decay curves of organic dyes in solution. A few attempts were made to use TCSPC in combination with scanning microscopes [34]. However,

the classic TCSPC technique was limited not only to relatively low count rates but also to slow scanning [33].

The situation changed with the introduction of the multi-dimensional TCSPC technique of Becker & Hickl. The new technique not only increased the recording speed by two orders of magnitude, it also added additional dimensions to the recording process. The photon distribution is recorded not only versus the time in the fluorescence decay but also versus the coordinates of a scanning area, the wavelength, or the time from the start of the experiment. The technique is extremely flexible, and the configuration of the hardware can be changed by a simple software command. Multi-dimensional TCSPC is described in detail in [18, 19].

TCSPC makes use of the special properties of high-repetition rate optical signals detected by a high-gain detector. Understanding these signals is the key to the understanding of TCSPC. The situation is illustrated in Fig. 5.

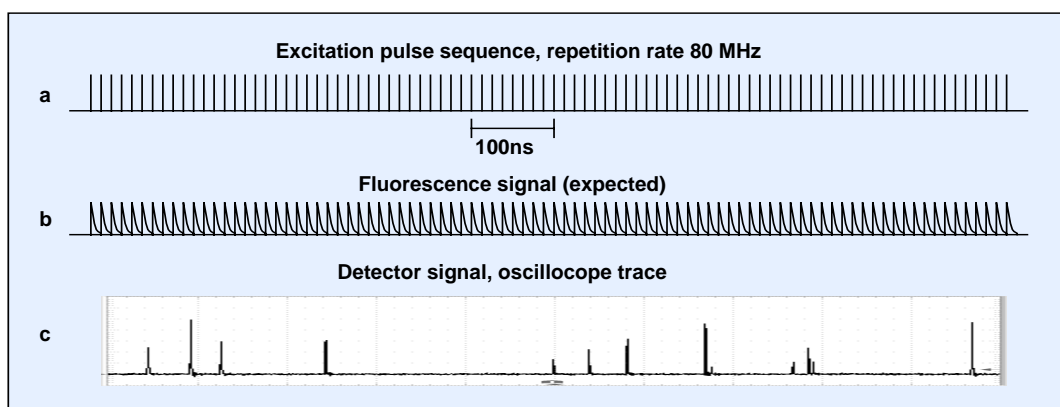


Fig. 5: Detector signal for fluorescence detection at a pulse repetition rate of 80 MHz

Fluorescence of a sample is excited by a laser of 80 MHz pulse repetition rate (a). The expected fluorescence waveform is (b). However, the detector signal measured by an oscilloscope has no similarity with the expected fluorescence waveform. Instead, it consists of a few pulses randomly spread over the time axis (c). The pulses represent the detection of single photons of the fluorescence signal. Please note that the photon detection rate of (c) is about 10^7 s^{-1} . This is on the order of the maximum possible detection rate of most detectors, and far beyond the count rates available from a living specimen in a scanning microscope. Thus, the fluorescence waveform (c) has to be considered a probability distribution of the photons, not anything like a directly observable signal waveform. Moreover, Fig. 5 shows clearly that the detection of a photon in a particular signal period is a relatively unlikely event. The detection of several photons in one signal period is even less likely.

The idea behind TCSPC is that only one photon per signal period needs to be considered. If only one photon needs to be detected per signal period the build-up of a photon distribution over the time in the signal period, and, in case of multi-dimensional TCSPC, over additional parameters is a straightforward task. Of course, the neglecting of a possible second photon and the resulting ‘pile-up effect’ are subject of never-ending discussion. It can, however, be shown, that the effect on the recorded lifetime under practical conditions is negligible [18].

The architecture of a multi-dimensional TCSPC device operated in the FLIM mode is shown in Fig. 6.

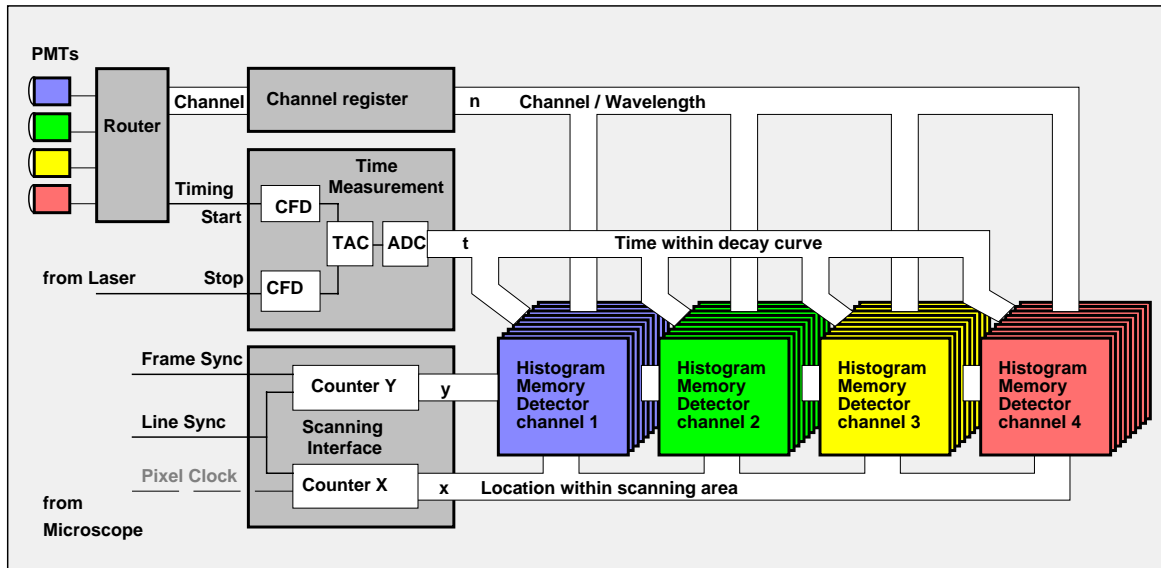


Fig. 6: Multidimensional TCSPC in the FLIM mode

At the input of the detection system are a number of photomultipliers (PMTs), detecting the fluorescence light from the excited spot of the sample in different wavelength intervals.

In the subsequent 'router' the single-photon pulses of the PMTs are combined into a common timing pulse line. The combination is possible because the photon count rate is considerably smaller than the repetition rate of the laser [18]. The timing pulse is sent through the time-measurement block of the TCSPC device. This block determines the time of the photon in the laser pulse period.

Along with the timing pulse, the router delivers the number, n , of the PMT in which a photon was detected. The detector number is stored in the 'channel register' of the TCSPC device. The detector number is used later to store the photons of the individual detectors in different memory blocks. The routing technique can be used with several individual PMTs [10, 13] and with multi-anode PMTs [15, 19]. A multi-spectral FLIM system based on a multi-anode PMT is available from bh [7]. The system is compatible with the RLD port of the Leica MP systems.

The scanning interface of the TCSPC module receives the scan clock signals from the scanning unit of the microscope. For each photon, the TCSPC module determines the location within the scanning area, x and y . The photon times, t , the detector channel number, n , and the spatial coordinates, x and y , are used to address a memory in which the detection events are accumulated. Thus, in the memory the distribution of the photon density over x , y , t , and n builds up. The result can be interpreted as a number of data sets for the individual detectors, each containing a large number of images for consecutive times in the fluorescence decay. The individual data sets can also be considered images with a fluorescence decay curve stored in each pixel.

The data acquisition runs at any scanning speed of the microscope. As many frame scans as necessary to obtain an appropriate signal-to-noise ratio can be accumulated. At the typical count rates obtained from living specimens the pixel rate is higher than the photon count rate. This makes the recording process more or less random; a photon is just stored in a memory channel according to its time in the fluorescence decay, its detector channel number, and the location of the laser spot in the sample in the moment of detection.

It should be noted that multi-dimensional TCSPC does not use any time gating, wavelength scanning, or detector multiplexing. For count rates up to several MHz virtually all detected

photons contribute to the result. Consequently, a near-ideal signal-to-noise ratio for a given fluorescence intensity and acquisition time is obtained.

The time resolution is determined mainly by the transit time spread of the detectors. With multichannel PMTs the width of the instrument response function (IRF) is about 30 ps (full width at half maximum, fwhm); for the standard detectors of the Leica FLIM systems about 150 ps are achieved.

The fluorescence decay curves in the individual pixels of the image are resolved into a large number - typically 64 to 1024 - time channels. The large number of time channels in combination with the near-ideal counting efficiency results in a near-ideal standard deviation of the measured fluorescence lifetime over a wide range of lifetimes [63]. Moreover, standard multi-exponential lifetime analysis techniques can be used to resolve complex decay profiles into their lifetime components and intensity coefficients.

It should also be mentioned that multi-dimensional TCSPC FLIM does not require any calibration by a lifetime standard. Lifetime standards are difficult to use because the effective fluorescence lifetime depends on the pH and the possible presence of fluorescence quenchers, see 'Fluorescence Quenching', page 2. In the Leica FLIM system the time scale of the TCSPC module is factory calibrated and the fluorescence decay is recorded into a large number of time channels; thus data analysis automatically delivers absolute lifetimes.

By a simple change of the operation mode (see 'Operation Mode', page 21) the TCSPC modules can be configured for a number of different signal recording procedures. In particular, the 'FIFO' or 'Time-Tag' can be used to simultaneously obtain fluorescence correlation (FCS) [24, 46, 87, 88], photon counting histograms (PCHs) [37, 78] and fluorescence decay curves in selected spots of a sample [18, 20]. The technique can even be used to identify the photon bursts of individual molecules and run a lifetime and anisotropy analysis with the bursts. The technique is termed 'Burst integrated fluorescence lifetime analysis, or BIFL [18, 44, 86, 96]

Sequential recording can be used to acquire fast triggered sequences of decay curves or even small images at high speed [19]. Typical applications are electro-physiology experiments or chlorophyll transients [51, 52, 76]. It should, however, be noted that most of these techniques are not finally explored in the Leica FLIM systems.

Thus, most FLIM systems actually use only a sub-set of the functionality of the TCSPC modules. In particular, many systems use only one detector. This may look surprising at first glance because several detection channels are standard in steady-state laser scanning systems. However, FLIM solves many problems without the need of multi-wavelength detection. For example, TCSPC FRET measurements resolve the interacting and non-interaction donor fractions from a single donor lifetime image. This is more than steady-state techniques with any number of spectral channels are capable of.

One-Photon FLIM versus Multi-Photon FLIM

As described above, FLIM requires a pulsed excitation source of both high repetition rate and picosecond pulse duration. In the Leica systems, this may be the Ti:Sapphire laser of a multi-photon microscope, or a picosecond diode laser. The corresponding FLIM systems are termed 'MP FLIM' and 'D FLIM' respectively. In terms of FLIM signal recording there is no difference between these systems. There are, however, differences in the way the sample is excited and the fluorescence light is detected. The MP FLIM uses two-photon excitation, the D FLIM one-photon excitation. This results in a number of optical differences which are discussed below.

The general optical principle of a laser scanning microscope is shown in Fig. 7. One-photon excitation is shown left, two-photon excitation right.

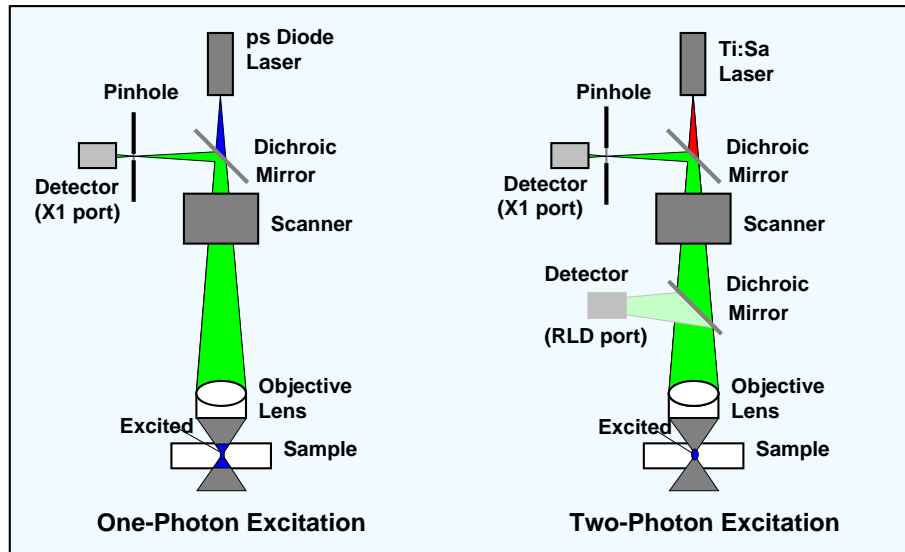


Fig. 7: One-photon FLIM (left) and multi-photon FLIM (right)

One-Photon Excitation With Confocal Detection

The laser is fed into the optical path via a dichroic mirror and focused into the sample by the microscope objective lens. Scanning is achieved by deflecting the beam by two galvanometer-driven mirrors. The excitation light excites fluorescence within a double cone throughout the whole depth of the sample. The fluorescence light from the sample goes back through the objective lens, and back through the scanner. After travelling back through the scanner the beam of fluorescence light is stationary. The light is focused into a confocal pinhole in an image plane conjugate with the image plane in the sample. Light from outside the focal plane is not focused into the pinhole and therefore substantially suppressed [41, 82, 100]. Out-of-focus suppression is the basis of the superior image quality and the optical sectioning capability of scanning systems. For FLIM out-of-focus suppression is even more important than for intensity imaging. Any mixing of the (possibly different) fluorescence lifetimes of different focal planes adds additional lifetime components to the apparent decay functions. The difficulties of unmixing lifetime components increase dramatically with the number of components. Out-of-focus suppression is therefore mandatory to obtain good FLIM results.

Two-Photon Excitation With Descanned Detection

With a fs Ti:Sa laser the sample can be excited by two-photon absorption [40, 50]. The efficiency of two-photon excitation increases with the square of the excitation power density. Noticeable excitation is therefore obtained only in the focus. Thus, two-photon excitation is a second way to obtain depth resolution and suppression of out-of-focus fluorescence, see Fig. 7, right. Different from one-photon excitation and confocal detection which avoids out-of-focus *detection*, two-photon excitation avoids out-of-focus *excitation*. Therefore, detection through a confocal pinhole is not required to obtain a good image quality. Nevertheless, feeding the fluorescence light back through the scanner and the pinhole often has benefits. The accuracy of FLIM can be seriously impaired by detection of background light and by optical reflections in the beam path. A pinhole, even if wide enough to transmit virtually all fluorescence light, yields substantial suppression of daylight and of optical reflections.

The standard FLIM configuration of the TCS SP2 is therefore descanned detection, with a fast FLIM detector attached to the 'X1 port' of the scan head.

Two-Photon Excitation With Direct Detection

In spite of the obvious benefits for FLIM, confocal detection in conjunction with two-photon excitation is not always feasible. Since the scattering and the absorption coefficients at the wavelength of the two-photon excitation are small the laser beam penetrates through relatively thick tissue. Two-photon excitation can therefore be used to excite fluorescence in tissue layers as deep as 1 mm [40, 65, 66, 83, 94, 95]. The problem is, however, that the fluorescence photons are strongly scattered on their way out of the sample and emerge from a relatively large area of the sample surface. Moreover, the surface is not in the focus of the objective. No matter which optical system is used, it is impossible to focus this light into a pinhole.

The solution to deep-tissue imaging is ‘direct’ or ‘non-descanned’ detection. The fluorescence light is diverted by a dichroic mirror directly behind the microscope lens and transferred into a detector, see Fig. 7, right. Thus, photons leaving the sample from a large area are collected and fed into the detector. Direct detection for the TCS SP2 and SP5 MP-FLIM systems is available as an option. It uses a fast FLIM detector at the ‘RLD port’ of the microscope.

Unfortunately the large detection area of a direct detection system has also a drawback: It increases the detection efficiency for scattered photons and for photons of background light similarly. Any direct detection system with TCSPC has therefore to be operated in *absolute darkness*.

It is often believed that non-descanned detection generally yields higher sensitivity than descanned confocal detection. This may be true for scan heads with poorly designed confocal detection paths. For the Leica SP it is clearly not the case. Thus, there is no need to use direct detection unless tissue thicker than 20 μm is to be investigated.

The Leica FLIM Systems

System Configuration

The FLIM systems are attachments to the TCS SP2 and SP5 microscopes. The principle is shown in Fig. 8.

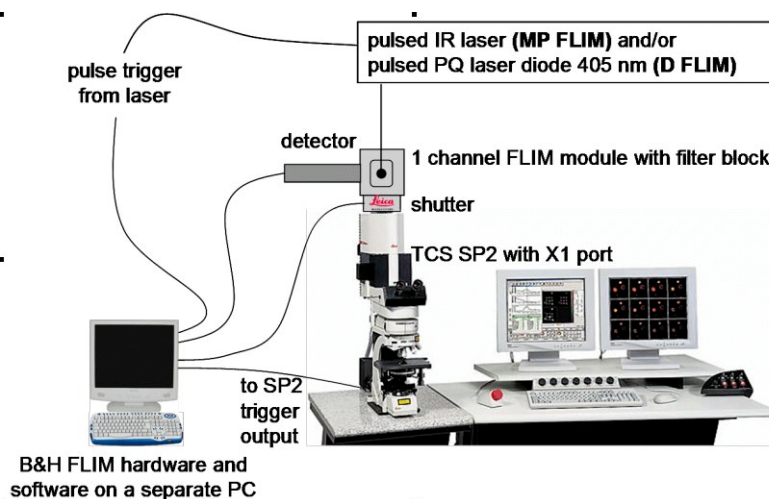


Fig. 8: System configuration of the Leica FLIM systems

The pulsed excitation is obtained either from the Ti:Sapphire laser of a multiphoton system or from a picosecond diode laser. The Ti:Sapphire laser is free-beam coupled to the SP2 scan head; the diode laser is coupled through a single-mode fibre. The wavelength of the Ti:Sapphire laser is tuneable from 710 nm to 890 nm, the wavelength of the diode laser is 405 nm.

Although the standard detectors of the SP2 scan head are sensitive enough to detect single photons their speed is not satisfactory for the typical FLIM application. Therefore a fast detector is attached to the 'X1 port' of the scan head. The standard detector is a PMC-100-0 of Becker & Hickl. The PMH-100-0 detector delivers an instrument response function (IRF) of about 150 ps width. Moreover, it features an extremely high IRF stability at high count rates [19]. Other detectors and dual-detector assemblies are available on special order.

For each detected photon, the detector delivers a pulse of about 1.5 ns width and about 100 mV amplitude (see Fig. 5). These single-photon pulses are fed into a Becker & Hickl SPC-830 TCSPC module [19]. Simultaneously, the SPC-830 modules receives reference pulses from the laser. For the Ti:Sapphire laser the reference pulses are generated by a photo-diode module within the laser safety box, for the diode laser they are obtained from the trigger output of the laser. Moreover, the TCSPC module receives scan clock pulses from the scan controller of the TCS SP2 microscope. From these signals the TCSPC modules derives the current position of the laser beam in the scanning area. The Y position within a frame is derived from a 'frame clock' and a 'line clock', the position within a by the times since the laser line clock.

Using these signals, the SPC-830 modules builds up a photon distribution over the time of the photons in the laser period and the coordinates of the scan area [18, 19], see 'Multi-Dimensional Time-Correlated Single Photon Counting', page 5.

The detector of the FLIM system is protected by a shutter. Both the detector and the shutter are controlled by a DCC-100 detector controller card (Becker & Hickl) [19]. The card provides power supply of the detector and its thermoelectric cooler, controls the detector gain,

and operates the shutter. When an overload occurs both the detector gain is shut down and the shutter is closed (see also DCC-100 S, page 18).

Both the SPC-830 and the DCC-100 module are operated in a computer separate from the computer of the TCS SP2. The FLIM system is controlled by its 'SPCM' data acquisition software, the TCS SP2 by its LCS software. The only connections to the TCS SP2 are the scan clock pulses, the cables of the detector and the laser synchronisation signal, and the shutter control cable. Thus, a FLIM upgrade does not set any restrictions to the functionality of the TCS SP2 or SP5.

SP2 Setup for FLIM measurement

All data acquisition parameters related to the TCS SP2 or SP5 are controlled by the Leica LCS software. The software panels shown in the following paragraphs are given for the TCS SP2. The settings apply analogously to the TCS SP 5. To start the system

- Turn on LCS computer.
- Start LCS Software.
- For general system handling, please, refer to the Leica LCS user manual.
- Choose FLIM laser (either pulsed 405 nm laser or MP laser), uncheck activation box (named 'active') for the continuous wave VIS lasers Ar/HeNe (2 in Fig. 2 and Fig. 4).

Laser Setup for D FLIM

- In laser control panel: click on control box '405 pulse'.
- Check box 'active' ('1' in Fig. 9).
- Set slider above '0.'

Remark: This slider does **not** control the intensity of the laser, it just displays the laser line in the spectrum. The intensity of the laser is controlled by the laser driver PDL 800-B.

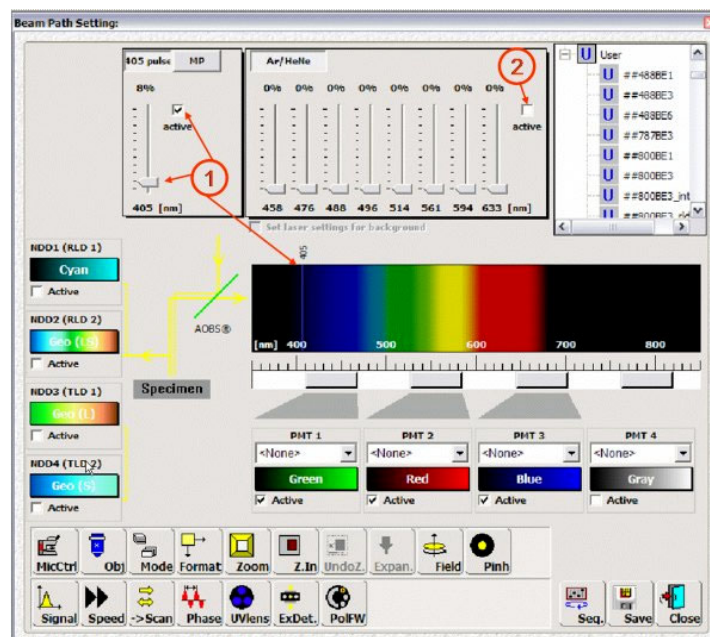


Fig. 9: LCS beam path window: Activation of 405 nm laser.

- Switch on laser driver PDL 800-B (power switch is on the rear side, 1 in Fig. 3).
- Turn key on left side on the front from 'STBY' to 'ON' (2 in Fig. 3).
- Set the trigger source on 'Int' (3 in Fig. 3).
- Set the intensity to a value between 3.5 and 10. (4 in Fig. 3)

- - Choose laser repetition frequency (5 in Fig. 3):
 - 1 = 40 MHz
 - 2 = 20 MHz
 - 4 = 10 MHz
 - 8 = 5 MHz
 - 16 = 2.5 MHz

For further Information, please refer to the user manual of the PDL800-B.

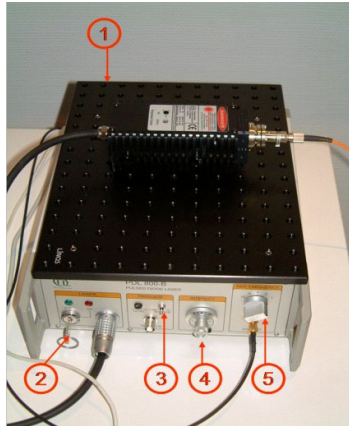


Fig. 10: PDL800-B Laser driver

Note: There are systems having both a diode laser and an MP laser available. Only one laser can be used for FLIM at a time. Please make sure the right Sync cable is connected to the SPC-830.

Laser Setup for MP FLIM

The MP laser is controlled by the LCS software, see Fig. 11.

- In laser control panel: click on control box 'MP'.
- Check box 'active' (1 in Fig. 11).
- Click on box 'Ctrl' (3 in Fig. 11).

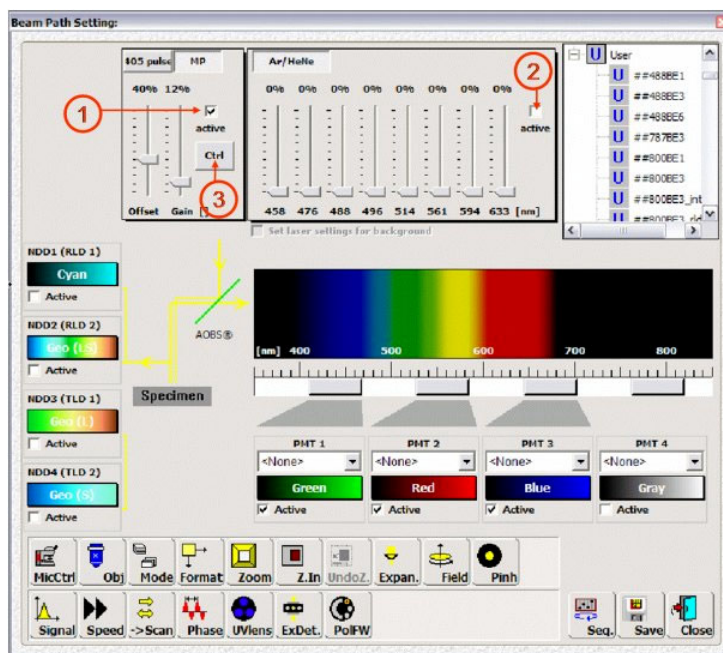


Fig. 11: LCS beam path window: Activation of MP laser

- A new control panel appears that is used to switch on and tune the laser, see Fig. 12.
- To start the laser, click several seconds on the control box 'standby' (1 in Fig. 12, left).
- The writing changes to 'laser on' and a green label 'pulsing' appears, indicating that the laser is now working in the mode lock (Fig. 12, middle).
- To open the shutter, click on the control box 'Shutter closed' (2 in Fig. 12, middle).
- The shutter opens, the box now says 'shutter open' and the laser safety sign appears (1 in Fig. 12, right).
- You can change now the wavelength either by moving the slider or by typing in the wavelength desired (2 in Fig. 12, right).

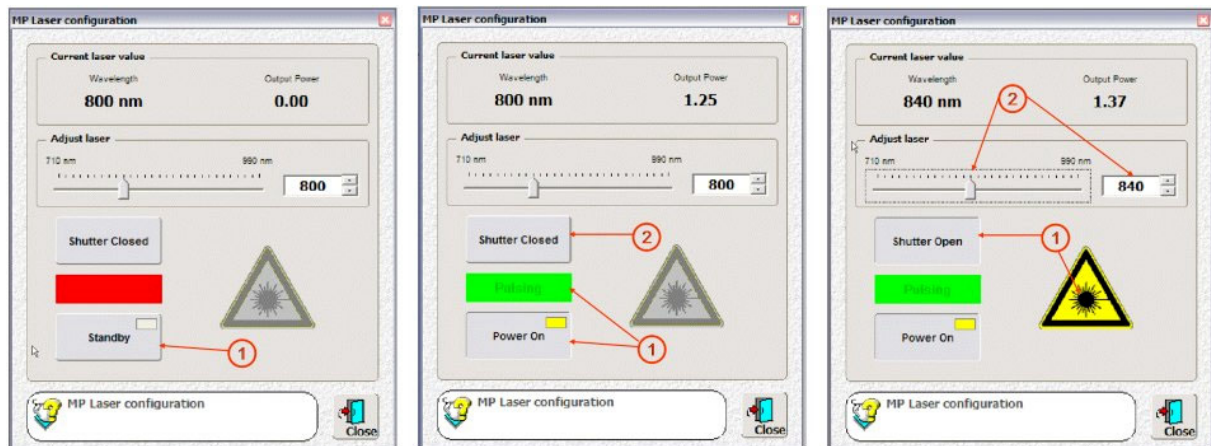


Fig. 12: Control panel MP laser configuration: Switch on MP laser (left), open shutter (middle), modify wavelength (right)

Note: There are systems having both a diode laser and an MP laser available. Only one laser can be used for FLIM at a time. Please make sure the right Sync cable is connected to the SPC-830.

Setup of Imaging Parameters in LCS Software

- Set Scan Speed = 400 Hz, unidirectional scan (1 and 2 in Fig. 13, left)
- Choose frame size (128x128, 256x256, or 512x512) (1 in Fig. 13, right)
- Set Mode = xyz (1 in Fig. 14, left)
- Set line average = 1 (1 in Fig. 14, right)
- Set pinhole size to 1 AU (Airy Unit) for D FLIM, open pinhole completely for MP FLIM (Fig. 15, left and right).
- Set polarisation filter wheel ('polFW', if present): The polFW allows blocking any IR light coming from the MP laser in MP FLIM. To select this option, choose the filter IRSP 715 or if this is not present BG 39 (1 in Fig. 14). For D FLIM choose an empty position.

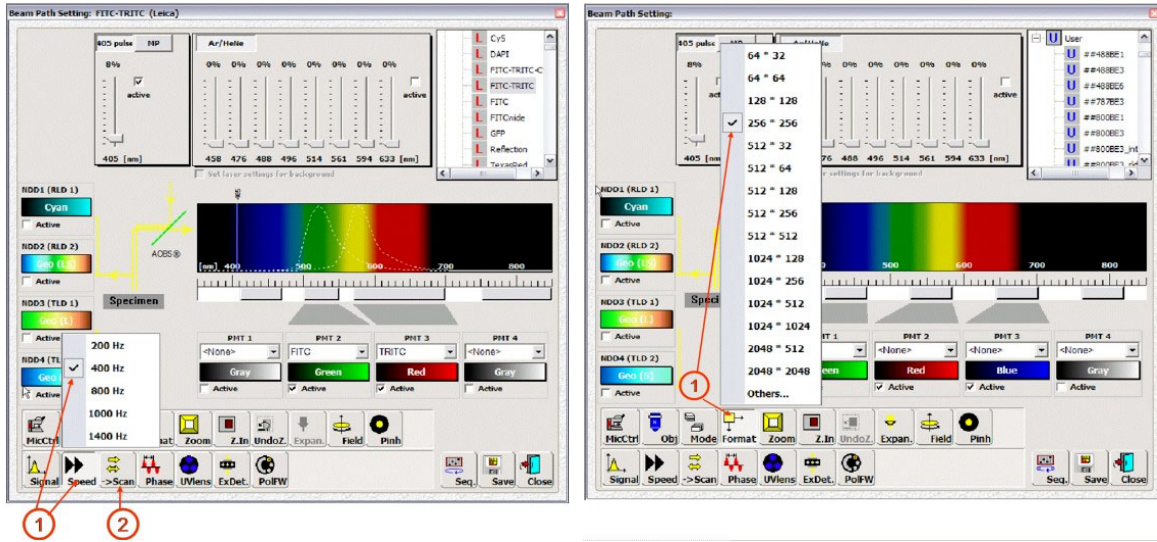


Fig. 13: LCS beam path window: Left: Definition of scan speed and unidirectional scanning mode. Right: Definition of image format

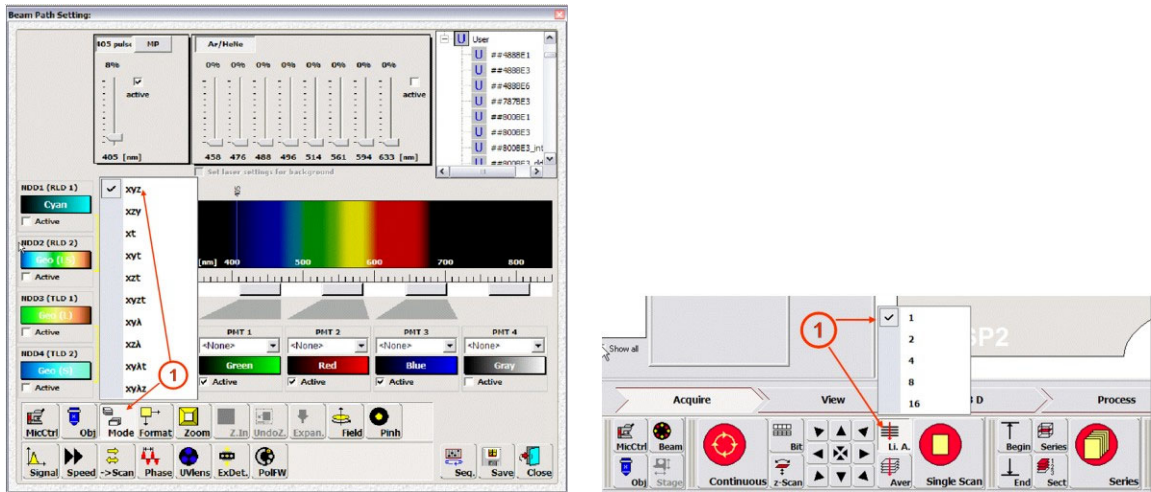


Fig. 14: Left: LCS beam path window, selection of imaging mode. Right: LCS main window, selection of line average.

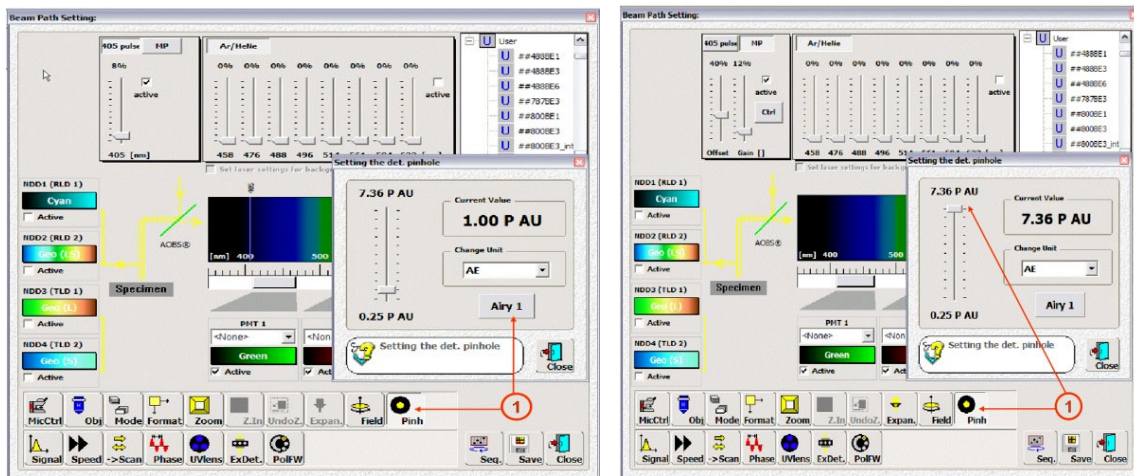


Fig. 15: LCS beam path window, setting the pinhole size. Left D FLIM, right MP FLIM

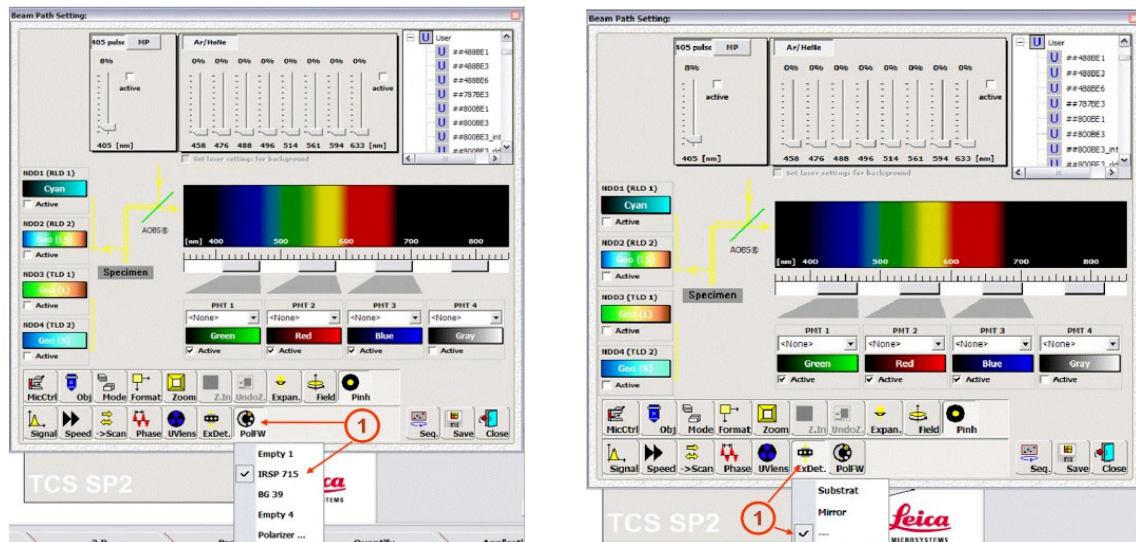


Fig. 16: LCS beam path window. Left: Setting the polarisation filter wheel containing the IR blocking filters. Right: Setting the slider position at external port

When the blocking filter is selected, proceed as follows:

- We recommend to take an xy overview image with internal detectors first and use it to set the desired zoom. For further explanations how to do this, please, refer to the LCS user handbook. If you are an experienced FLIM user you may skip this step and record an overview image in the life mode of the FLIM module, see 'Repeat Function', page 22.
- Set the external port 'ExDet' on position '--' (1 in Fig. 16, right). Thus the fluorescence photons do not reach the internal PMTs, but the FLIM detector only. Correspondingly, no images with internal PMTs can be obtained.
- Now the SP2 is ready for FLIM data acquisition.
- To come back to 'normal' intensity imaging with internal detectors set the extDet to 'Mirror'. If you choose the position 'Substrate' 90% of the light go to the FLIM detector and 10% to the internal detectors.

Scanning a Sample

The recording of FLIM data is based on concerted operation of the TCS SP2 microscope and the SPC-803 TCSPC module. Controlled by its LCS software, the TCS SP2 microscope scans the sample. The photons detected by the FLIM detector are processed in the TCSPC module, which is controlled by its SPCM software. The data acquisition in the TCSPC modules is synchronised with the scanning by two scan clock signals, see Fig. 6, page 7.

Please note that recording reasonable FLIM data normally requires accumulation of the photons over a large number of frames. Therefore a 'continuous scan' must be used.

To enable the TCS SP2 to run a scan one of the internal detectors needs to be activated, even if it is not used for data acquisition (2), see Fig. 17. The scan is started and stopped by clicking on the start/stop button (1).

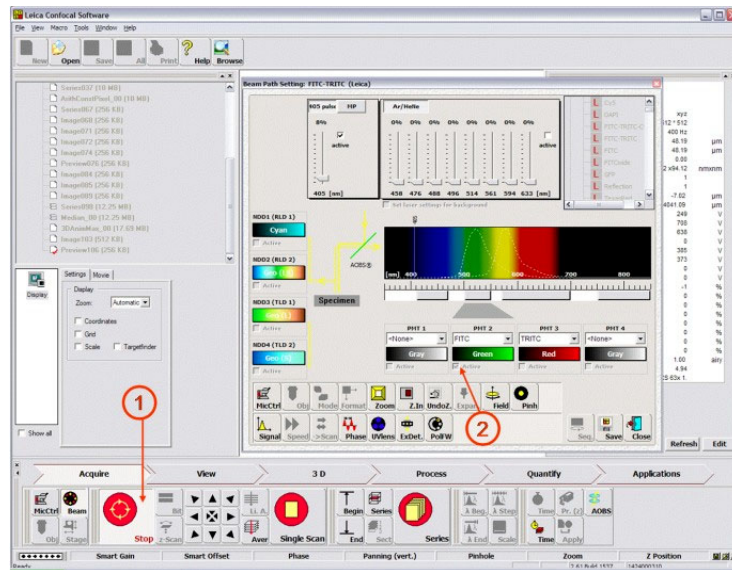




Fig. 17: LCS main window during FLIM data acquisition. The scan is started and stopped by clicking on the start/stop button (1). At least one of the internal detectors must be active to enable scanning (2)

To scan a sample with FLIM data acquisition

- Activate one or several internal detectors to enable scanning (2).
- Start a continuous scan in the microscope by clicking on the  (continuous scan) button (1), see Fig. 17.
- Adjust the laser power to obtain reasonable count rates (see ‘Details of FLIM Data Acquisition’, page 33), and start the measurement in the SPCM software (see ‘Steps of a FLIM Measurement’ page 31).
- Let the SPCM software finish the recording, or stop the FLIM measurement manually.
- Stop the scan in the microscope by clicking on the  button, see Fig. 17.

The procedure is tolerant against operator errors. You may first start the FLIM measurement and then the scan. The SPC-830 module then simply waits until the scan starts. Only if you do not start the scan within the ‘collection time’ defined in SPCM the SPC-830 will give up. You may also stop the scan in LCS while the FLIM measurement is still running. The FLIM measurement simply stops recording photons and waits. You can stop the FLIM measurement at any time without creating artefacts. After an operator stop command the measurement will automatically continue for the current frame so that recording incomplete frames is avoided.

With the LCS settings recommended in Fig. 16, right, all photons are directed to the FLIM detector. Alternatively, you may direct a small fraction of the light to the internal detectors by setting ‘ExDet.’ to ‘Substrate’.

FLIM Data Acquisition Software

The FLIM system is controlled by the ‘SPCM’ software of the SPC-830 module and by the software of the DCC-100 detector controller. To start the software

- Turn on FLIM computer
- Start the DCC-100 and the SPCM application. On startup, both applications run a hardware test and show the startup windows shown in Fig. 18. Both panels should indicate ‘Hardware Mode’ and display a valid serial number and PCI address.
- Click on OK (2) to start the main panels of both applications.

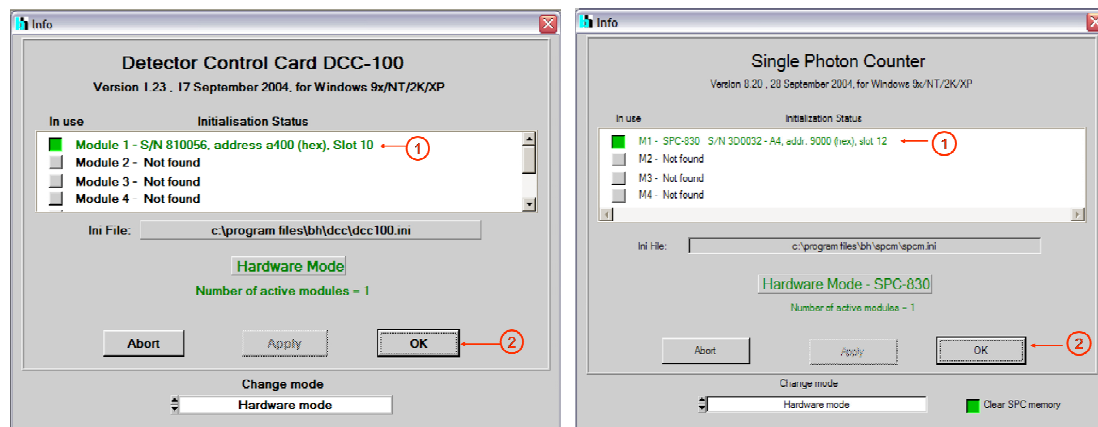


Fig. 18: Startup panels of DCC software (left) and SPCM software (right)

DCC-100 Software

The main panel of the DCC software is shown in Fig. 19. The DCC-100 card has three interface connectors, two for controlling detectors or lasers, and one for controlling shutters, see [8, 19]. In the standard configuration of the Leica FLIM systems the detector is controlled via connector 3, the shutter via connector 2.

- Resize the DCC to a convenient format and place it in a convenient part of the screen (see SPCM main panel, Fig. 20). To keep the panel visible when other applications are opened, we recommend to click into ‘Parameters’ and activate ‘Always on Top’.
- Make sure that the boxes for power supply of detector (12 V, 1 in Fig. 19, left), shutter (12 V, 2 in Fig. 19, left) and cooling (3 in Fig. 19, left) are activated. The DCC software automatically starts with the settings used in the last session, therefore there is usually no need to change the setup.
- For the PMC-100 FLIM standard detector, set the gain of the detector to a value between 90 and 100 % (in Fig. 19, left, (4)). Please note that the gain of a photon counting detector cannot be reasonably used to change the intensity of the recorded image. Please see [19].
- Click on the ‘Enable Outputs’ button to enable the detector, see Fig. 19, middle, (2).
- Before you start a measurement, open the shutter by clicking on the ‘b1’ button (1).

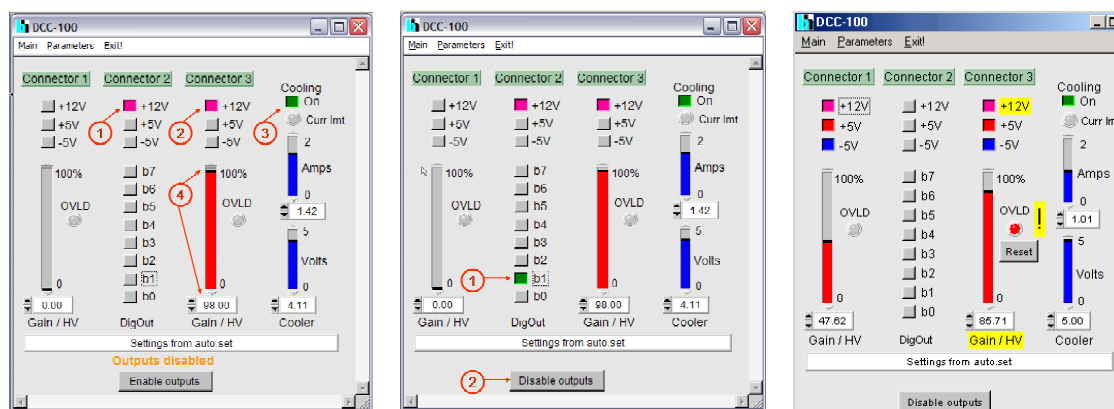


Fig. 19: DCC 100 main panel. Left: After startup, detector(s) and shutter disabled. Middle: Detector enabled and shutter open; ready for data acquisition. Right: Detector shut down by overload.

If the light intensity on the detector is too high the DCC-100 closed the shutter and shuts down the detector. The situation is shown in Fig. 19, right. In this case, reduce the light intensity, click on the 'Reset' button, and click on 'b1' to open the shutter again.

SPCM Software

The SPCM software allows the user access the full functionality of all Becker & Hickl TCSPC modules [19]. In particular, there are operation modes for recording single decay curves, time-controlled sequences of decay curves simultaneously for several detector channels, fluorescence correlation and photon counting histogram data, FLIM images in several detector channels, multi-wavelength FLIM images, or sequences of FLIM images. Although this is not tested in details, most of these features can potentially be used in conjunction with the Leica TCS SP2 microscopes. The SPCM software therefore contains by far more system and measurement control parameters than you need for recording a FLIM image in a single detector channel. Depending on the application different, often multi-dimensional results are to be displayed. The main panel of the SPCM software can therefore be configured by the user.

Please do not get confused by the variety of options. The SPCM software stores the complete set of system, control, and configuration parameters. Thus, all you have to do to configure the system is to load the right setup files delivered with your FLIM system. Moreover, the setup data are included in the measurement data files. You may therefore also load the data file of a successful measurement and run a new measurement with exactly the same parameter set.

The main panel of the SPCM software is shown in Fig. 20. As mentioned above, the panel is configurable by the user, see [19], 'Configuration of the SPC Main Panel'. For standard FLIM application we recommend to keep the 'Display Parameters' open as shown in Fig. 20. We also recommend to keep the DCC panel open and place it in the lower right part of the screen.

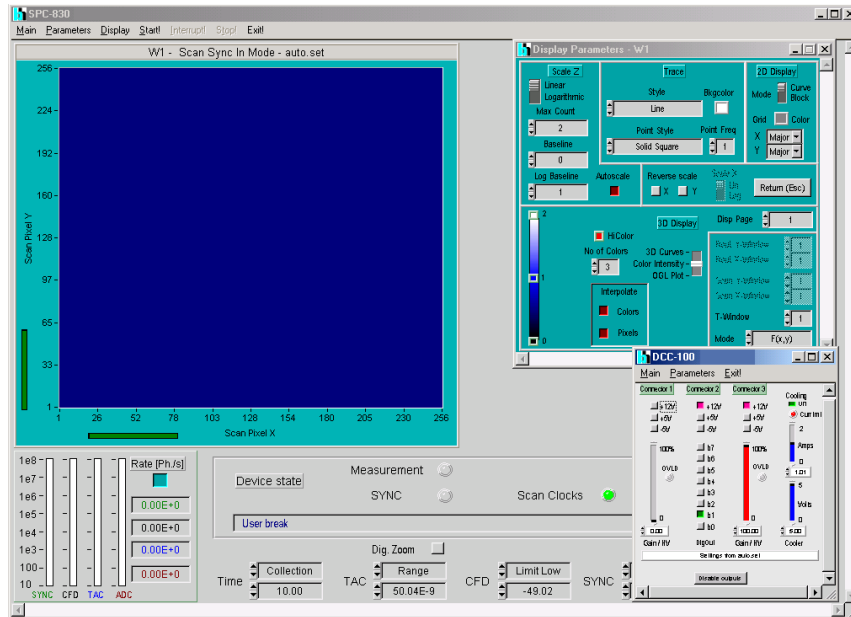


Fig. 20: SPCM main panel with display parameter panel open and DCC panel placed in lower right corner

TCSPC System Parameters

The ‘System Parameters’ contain the complete set of hardware and measurement control parameters of the TCSPC module. Please note that the setup files delivered with your FLIM system contain reasonable system parameters. Thus, there is usually no need to change anything in these settings. The following paragraph should therefore be considered supplementary information for advanced users.

The system parameters are accessible by clicking into ‘Parameters’, ‘System Parameters’. The system parameter panel is shown in Fig. 21.

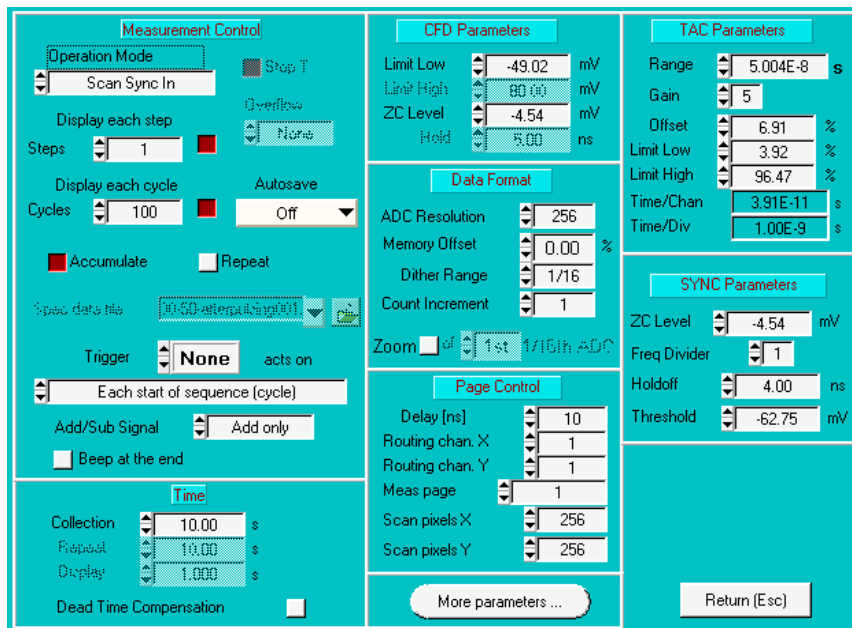


Fig. 21: System parameter panel

A detailed description of the system parameters is given in [19]. An overview is given in the following paragraphs.

Measurement Control Parameters

Operation Mode

The operation mode selection panel of the SPC-830 TCSPC modules are shown in the figure right. The mode used for FLIM recording is ‘Scan Sync In’. Other modes may be used for special application of a FLIM system:

The ‘*Single*’ mode records one decay curve for each of the detectors connected to the SPC-830 module. It can be used for fluorescence decay measurement with the laser beam being parked in a pixel of interest. If used in combination with scanning it delivers an average decay curve over the complete scan area.

The ‘*Oscilloscope*’ mode performs a repetitive measurement and displays the results like an oscilloscope. The mode is an excellent tool for setup, maintenance and alignment purpose.

The $F(t,T)$ mode runs a time-controlled sequence of ‘*Single*’ measurements. It is useful for photobleaching experiments, experiments of photodynamic therapy, and for recording chlorophyll transients.

The $F(t,EXT)$ mode is implemented for recording sequences of curves in connection with external experiment control. The $F_i(T)$ and $F_i(EXT)$ modes record time-gated intensity curves. There is no reasonable application of these modes in a scanning microscope.

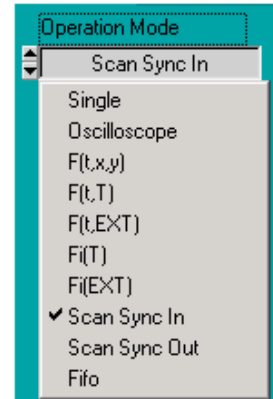
The ‘*Scan Sync In*’ mode is the mode for recording FLIM data in a scanning microscope. The SPC-830 module records a photon distribution over the time in the laser period and over the coordinates of the scan area, see Fig. 6, page 7.

‘*Scan Sync Out*’ is an imaging mode that actively controls a scanner. It is implemented mainly for scanning with piezo-driven scan stages. However, the Scan Sync Out mode can also be used to record and accumulate fast triggered sequences of decay curves. With a large number of accumulation cycles sequences as fast as a few microseconds per curve can be recorded. The mode can be used to record photochemical quenching transients in chlorophyll [18], possibly also effects of electro-physiological stimulation in neurones. Please see [19] for details.

The ‘*FIFO*’ mode differs from all the other modes in that it does not build up any photon distribution. Instead, the FIFO mode stores information about each individual photon. This information stored is the time in the laser period, the time since the start of the experiment, and, if several detectors are used, the number of the detector that detected the photon. The FIFO mode is the key to the application of single-molecule techniques. It can be used to record FCS curves in combination with fluorescence decay curves, photon counting histograms, or BIFL (burst-integrated fluorescence lifetime) data [18, 20, 44, 46, 86]. These techniques require parking the beam with extremely low beam jitter and a detection volume on the order of a femtoliter. Although this is possible in the Leica TCS SP2 the techniques are not tested in detail yet. For details please see [19]; typical results are described in [18].

Steps and Cycles

The memory of the SPC modules provides memory space for a large number of decay curves, or even for several measurements containing many decay curves each. In particular, there may be enough space to store the data of a large number of images with moderate numbers of pixels and time channels. The individual memory blocks are termed ‘pages’. By defining a number of ‘steps’ greater than one a sequence of recordings can be defined that automatically steps through subsequent pages.



A measurement sequence may also be defined with several ‘cycles’. The results of the individual cycles can either be accumulated (‘accumulate’ button) or read from the device memory and automatically saved into subsequent data files (‘autosave’). The functions can be used for on-line display during a FLIM measurement, see Fig. 24, page 24. Moreover, they can be used to record and save a number of subsequent recordings taken from the same sample.

Repeat Function

By activating the ‘repeat’ button the complete measurement cycle is repeated until it is stopped by a user interaction.

The repeat function can be used to create a ‘Life Mode’ of TCSPC imaging. The image is defined with a moderate number of ‘scan pixels X’ and ‘scan pixels Y’, and an ADC resolution of ‘one’. With one ADC channel the recorded image is a pure intensity image of moderate data size. This keeps the time for the data readout on a negligible level. With a fast scan rate and a collection time on the order of 1 second a sufficiently fast update rate for adjusting the focus or selecting an image area of the sample is obtained.

Trigger

The start of a measurement, the steps of a page stepping sequence, or the cycles of a measurement sequence can be triggered. Please see [19].

Collection Time

Collection time is the acquisition time for the measurement, or, of page stepping or cycling is used for each step or cycle of a measurement. With the parameters shown in Fig. 21 100 cycles of 10 seconds are performed, with the results being accumulated and displayed after each cycle. It is not required that you run a FLIM measurement over the full collection time or the full number of cycles. If you are satisfied by the signal-to-noise ratio you can stop the measurement at any time. After an operator stop command the internal scanning machine completes the current frame, so that artefacts by accumulating incomplete frames are avoided.

CFD, SYNC and TAC Parameters

These parameters control the constant fraction discriminators at the inputs of the detector and laser synchronisation signal, and the time conversion circuitry in the TAC. You may possibly change the conversion range of the TAC by changing TAC gain and TAC offset. In case of synchronisation problems (indicated by wrong SNYNC rate) you may also attempt to change ‘SYNC Threshold’. In general, we discourage changing these parameters unless you are familiar with the TCSPC hardware. Please see [19] for details.

Data Format and Page Control

ADC Resolution is the number of time channels in the decay curves recorded. For FLIM recording there is also a conjunction between the available number of pixels and the available ADC resolution. The maximum ADC resolution is 4096, the minimum ‘one’. ADC resolution = 1 does, of course, not yield any time resolution. It can, however, be used to obtain life-display of images for adjusting a sample, the focus, or the region of interest of the scan. Unless you want to run life display or a page stepping sequence we recommend to use the highest ADC resolution available.

Scan Pixels X and Scan Pixels Y are the number of pixels of the FLIM Image. Please note that several adjacent pixels of the SP2 or SP5 scan may be binned into one pixel of the FLIM data, see Fig. 22. Scan Pixels X and Scan Pixels Y may therefore be smaller than the pixel numbers

of the scan defined in the LCS software. There is also a conjunction between the available number of pixels and the available ADC resolution.

For other data format and page control parameters, please see [19].

Scan Parameters

The image acquisition in the SPC-830 module is synchronised with the scan in the microscope via the scan clock pulses (see Fig. 6, page 7). In the SP5 the synchronisation works via the frame clock, line clock and pixel clock signals, in the SP2 only via a frame clock and a line clock signal. Moreover, several adjacent pixels of the SP2 or SP5 scan may be binned into one pixel of the FLIM image. The details of the synchronisation are defined under ‘More parameters’.

‘More Parameters’ are hardware setting that are specific for the selected operation mode. In the Scan Sync In mode used for FLIM the ‘more parameters’ panel contain the scan control and pixel binning parameters, see Fig. 22. You may change these parameters to create FLIM image sizes different from the sizes defined in the setup files delivered with the system. It should, however, be noted, that changing these parameters requires some knowledge about the scanning hardware. Please refer to [19] and save a setup file of the current settings before you make any changes.

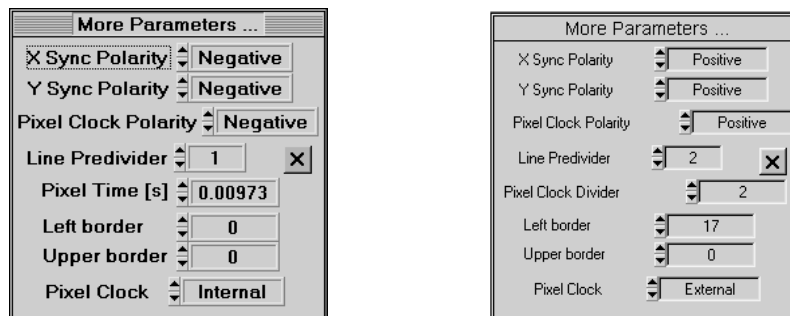


Fig. 22: Scan parameters. Left: SP2, the FLIM data acquisition works with internal pixel clock. Right: SP5, the pixel clock of the microscope is used as an external pixel clock of the FLIM data acquisition.

Access of System Parameters from Main Panel

To facilitate on-line adjustments the essential hardware and measurement control parameters are also accessible directly from the main panel, see Fig. 23.

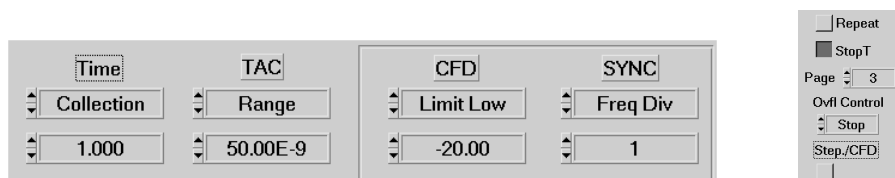


Fig. 23: Access to system and control parameters from main panel

Display of Images in the SPCM Software

Online Display

Images can be displayed at the end of a FLIM measurement or in regular intervals within the measurement. On-line display is achieved by defining a large number of measurement ‘cycles’ and activating ‘accumulate’ and ‘display each cycles’ in the system parameters of the SPCM software. See figure right. The setting shown runs 100 cycles of the specified ‘collection time’, accumulates the data, and displays the accumulated data after each cycle. The display of the data itself is controlled by the ‘Display Parameters’ and ‘Window Parameters’, see paragraphs below.

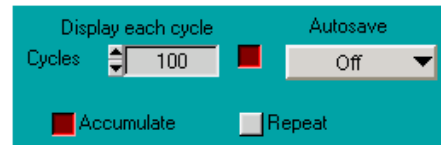


Fig. 24: On-line display

Display Parameters

The data recorded by the FLIM system are multi-dimensional. There is a two-dimensional array of pixels, and each pixel contains a photon numbers in a large number of time channels within the laser period. Each pixel may even contain such data for a number of different wavelength channels, or for different times from the start of the experiment. The SPCM software is able to display such data in various display modes, see [19]. The display is controlled by the ‘Display Parameters’. The display parameters recommended for FLIM acquisition with a single detector are shown in Fig. 25.

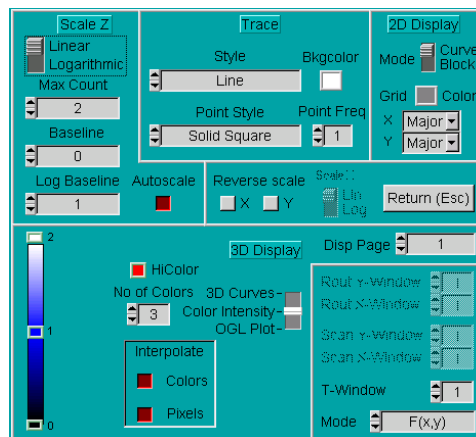


Fig. 25: Display parameter panel of the SPCM software

A detailed description of the display parameters and their influence on the display of multi-dimensional TCSPC data is given in [19]. The parameters important for the standard configurations of the Leica FLIM systems are briefly described below. Please note that the setups coming with you FLIM system contain reasonable display parameters. The following paragraphs should therefore be considered supplementary information for advanced users.

Scale Section

- Linear/Logarithmic: Defines a linear or logarithmic intensity scale. For displaying FLIM images we recommend ‘linear’.
- Max Count, Baseline: Display range (in photon counts) for linear display
- Log Baseline: Lower display threshold for logarithmic display
- Autoscale: Sets Max count automatically according to maximum number of photons in the displayed data. For FLIM we recommend ‘Autoscale ON’.

- Reverse Scale: Images can be reversed both horizontally and vertically.

3D Display Section

- 3D Curves / Colour Intensity / OGL Plot: Displays data as a sequence of curves, as an image, or as a curved surface. For FLIM use 'Colour Intensity'.
- Colour Bar: Assigns colours to the photon numbers in the pixels of the Colour-Intensity display.
- Interpolate Colours / Pixels: Switch on for FLIM.
- HiColour: Colour assigned to pixels with photon numbers out of the display range. Please note that HiColour only indicates that these pixels cannot be displayed within the display scale used. The corresponding pixels are usually *not* saturated.
- Display page: A measurement can contain several smaller images recorded consecutively. These images are contained in different 'pages' of the device memory.

Selection of subsets of multidimensional data

- T Window: TCSPC data can be multi-dimensional data cubes, but only one plane through the cube can be displayed at a time. For FLIM measurements with a single detector images in selectable time windows are displayed. The time window are defined in the 'Window Intervals', see below.
- Mode: Defines the plane through the multidimensional data cube. For FLIM images, use $f(x,y)$.

Window Parameters

The display routines of the SPCM software display subsets of multi-dimensional data arrays. These can be images within specified time windows or ranges of detector channels, decay curves along one coordinate within a spatial interval of the other coordinate, time-controlled sequences of waveforms within a range of detector channels, or intensity values along a one-dimensional scan within specified time windows. The required window definitions are provided by the 'Window Intervals', see Fig. 26.

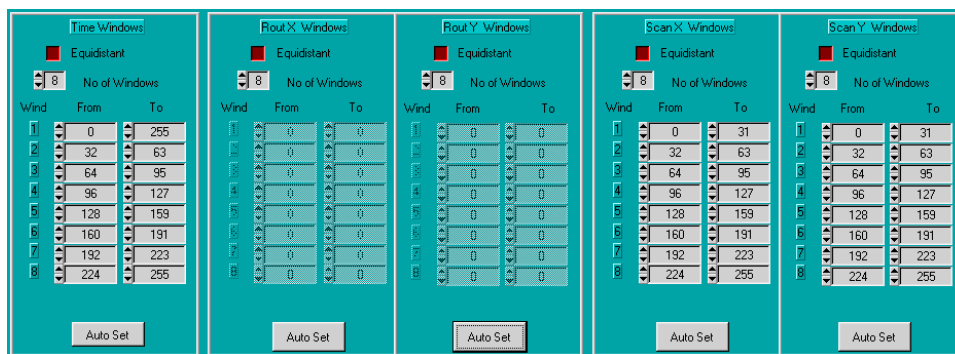


Fig. 26: Window parameters

The 'Time Windows' are used for calculating integral photon numbers in selected time intervals of decay curves or other waveforms. The definitions shown in Fig. 26 are for FLIM display of images recorded with an ADC resolution of 256 time channels. Eight time windows are provided. The first window covers all time channels. An image displayed in this window contains all photons, i.e. is a pure intensity image. The following windows are consecutive time gates within the laser period. Images in these time windows are gated images, as you can see by stepping through the 'T Windows' of the Display Parameters (Fig. 25).

The Scan X and Scan Y windows are used to display decay data over selectable stripes of an image. Please see [19].

The Routing X and Y windows are used to select data from an array of detectors in a multi-detector setup. Because the standard FLIM system has only one detector the routing windows are disabled. They are, however, used to select the detector channels of a dual-detector system or to define wavelength intervals in multi-wavelength FLIM systems, see 'Special FLIM System Configurations', page 50.

Please note that the Window parameters are different for different numbers of pixels or time channels. When these parameters are changed the SPCM software automatically calculates new window parameters.

Saving Setup and Measurement Data

The ‘Save’ panel is shown in Fig. 27. It contains fields to select different file types, to select or specify a file, to display information about existing file, and to select between different save options.

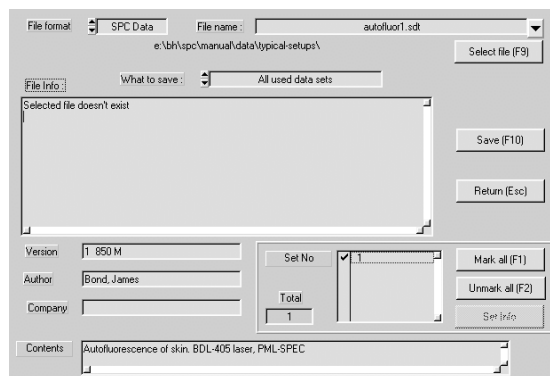



Fig. 27: Save panel

File Format

You can choose between ‘SPC Data’ and ‘SPC Setup’. The selection refers to different file types. With ‘SPC Data’ files are created which contain both measurement data and system parameters. When this file is loaded not only the measurement data are restored but also the complete system setup. With ‘SPC Setup’ files are created that contain the system parameters only. When such files are loaded the system setup is restored, but no data are loaded. Files created by ‘SPC Data’ have the extension ‘.sdt’, files created by ‘SPC Setup’ have the extension ‘.set’.

File Name / Select File

A file name can be written into the ‘File Name’ field. ‘Select File’ opens a dialog box that allows you to change or create directories. Moreover, it shows the names of existing files. These are ‘.sdt’ files or ‘.set’ files, depending on the selected file format. If you want to overwrite an existing file you can select it in the ‘File Name’ field. A history of previously saved files is available by clicking on the  button.

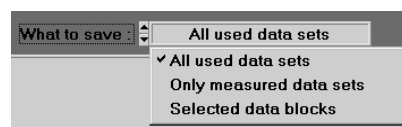
File Info

After selecting the file text can be written into the ‘Author’, ‘Company’ and ‘Contents’ fields. Both for ‘SPC data’ and ‘SPC setup’ the file information is saved in the file. The file information helps considerably to later identify a particular measurement among a large number of data files. We therefore strongly recommend to spend a few seconds on typing in a reasonable file information.

If you have selected an existing file the file information contained in it is displayed in the ‘File info window’. If you want to overwrite this file you can edit the existing file information.

Selecting the data to be saved

Under ‘What to Save’ the options ‘All used data sets’, ‘Only measured data sets’ or ‘Selected data blocks’ are available. The default setting is ‘All used data sets’, which saves all valid data available in the memory of the SPC



modules. These can be measured data, calculated data or data loaded from another file. *Except for special cases (see[19]) we recommend to use the ‘All used data sets’ option.*

Loading Setup and Measurement Data

The 'Load' menu is shown in Fig. 28. It contains fields to select different file types, to specify a file, to display information about the file selected, and to select different load options.

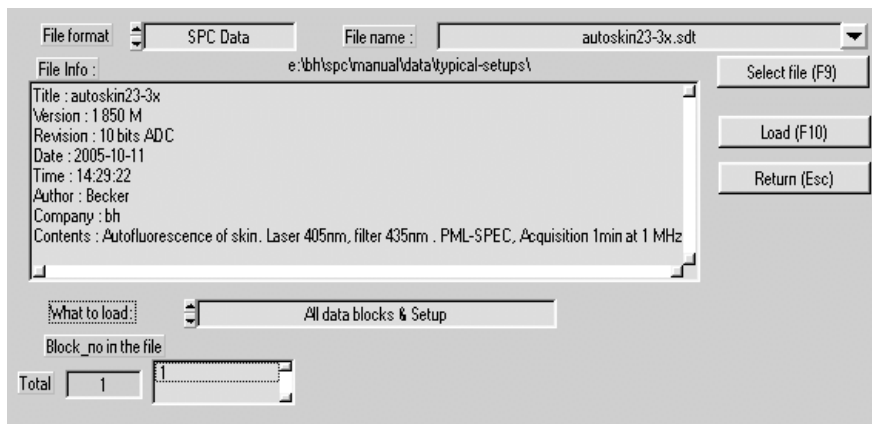


Fig. 28: Load panel


File Format

You can choose between 'SPC Data' and 'SPC Setup'. The selection refers to different file types. With 'SPC Data', .sdt files are loaded. These files contain both measurement data and system parameters. Thus the load operation restores the complete system state as it was in the moment when the file was saved.

If you choose 'SPC Setup', .set files are loaded. These files contain the system parameters only. The load operation sets the system parameters, but the actual measurement data are not influenced.

Note: Measurements in the 'FIFO' (time tag) mode deliver an .spc file that contains the micro time, the macro time, and the detector channel for each individual photon. These files are loaded by using the 'Convert' routines, see [19].

File Name / Select File

The file to be loaded can be selected in the 'File Name' field. 'Select File' opens a dialog box that displays the available files. These are '.sdt' files or '.set' files depending on the selected file format. A history of previously loaded files is available by clicking on the  button.

File Info

The file info window displays information about the file selected. The first three lines of the file info are inserted automatically when a file is saved. The last three items can be typed in by the operator, see 'Saving Setup and Measurement Data'.

Block Info

Activating a data block in the 'Block Number in File' field enables a 'Block Info Button'. Clicking on this button opens a list that contains the device number of the SPC modules by which the data were recorded, the time and date of the recording, and all system parameters, see Fig. 29. At the end of the block information the minimum and maximum count rates of the corresponding measurement are shown (see Fig. 29, right). The block info often helps to recover the exact recording conditions of an older measurement.

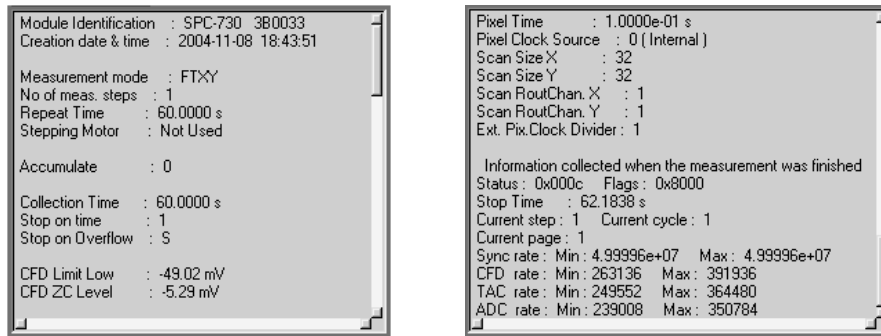


Fig. 29: Block info window of the load panel

Load Options

Under ‘What to Load’ the options ‘All data blocks & setup’, ‘Selected data blocks without setup’ or ‘Setup only’ are available. The default setting is ‘All data blocks & setup’, which loads the complete information from a previously saved data file. *Except for special cases (see below) we recommend to use the ‘All data blocks & setup’ option.*

Loading Files from older Software Versions

Older software versions may contain less system parameters than newer ones. Therefore, loading older files into a newer software (or vice versa) can cause warnings of missing or unknown parameters. To load the file, click on the ‘Continue’ button until the file is loaded. Unknown parameters are ignored, and missing parameters are replaced with default values. To avoid further problems with such a file, we recommend to save it in the current software version (Use option ‘All used data blocks’, see ‘Saving Setup and Measurement Data’).

Setup Files Delivered with the FLIM System

The setup file holds the information of scan speed, image format and laser repetition rate. Because this information is not transferred from LCS automatically, the right configuration file must be selected.

- To load the configuration file, click on Main, Load, see Fig. 30 (1).
- In the new window chose file format ‘SPC setup’, see Fig. 30 (2).
- Click on ‘Select file’ see Fig. 30 (3).
- A path is shown. The name of the folder indicates whether the setup files are for D FLIM or MP FLIM see Fig. 30, left and right.
- Navigate to the correct folder. Choose the file of the desired configuration, double click on it, see Fig. 30 (4) and click on ‘Load’, see Fig. 30 (5).

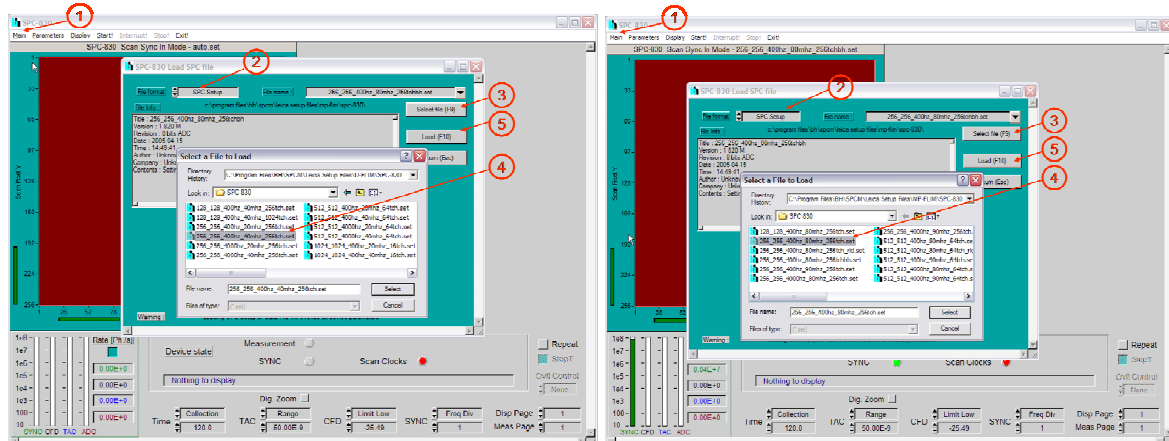


Fig. 30: Loading of D FLIM setup files (left) and MP FLIM setup files (right).

The general nomenclature of the file names is:

(Pixel number)x(Pixel number)_(Scan Speed)_(Laser repetition rate)_(number of time channels).set

Example:

File name:	256x256_400hz_40mHz_512tch.set
Frame size:	256x256
Scan speed:	400 Hz
Laser repetition rate:	40 MHz
Number of time channels per pixel:	512

Predefined Setups

Setups of frequently used system configurations can be added to a list of ‘predefined setups’. Changing between these setups then requires only a mouse click.

To use the predefined setup option, click on ‘Main’, ‘Load Predefined Setups’. This opens the panel shown in Fig. 31, left. A setup is loaded by clicking on the button left of the name of the setup.

To add or delete setups to or from the list, or to change the names of the setups, click into one of the name fields with the right mouse key. This opens the panel shown in Fig. 31, right. To add a setup, click on the disc symbol right of the ‘File Name’ field and select a ‘.set’ file. Default setups coming with the SPCM software are in the ‘default setups’ folder of the working directory defined during the software installation. Please note that there may be sub-directories for different classes of applications. Select the files you want to put into the list of predefined setups, and click on the ‘Add’ button. Every setup has a user-defined ‘nickname’. The default nickname is the file name of the .set file. To change the nickname, click into the nickname field and edit the name. Then click on ‘Replace’.

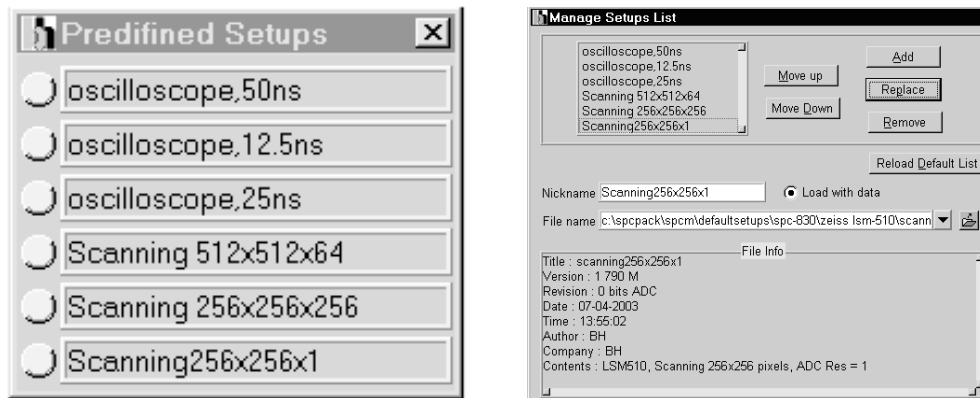




Fig. 31. Left: Panel for loading predefined setups. Right: Editing the list of predefined setups

To create your own predefined setups, first save a setup file of the system configuration you want to add the list. Use the ‘Save’ panel, option ‘setup’, as described under ‘Save’. Then add the file to the setup list as described above.

You can also add an ‘.sdt’ file to the setup list. The .sdt file contains not only the system settings but also measurement data. You can define whether the file is loaded with or without the data by clicking on the ‘load with data’ marker. Please note that loading files with data can take a longer time than without, especially for data recorded in the FLIM mode of the SPC-830.

FLIM Measurements

Steps of a FLIM Measurement

- (1) Turn on the computer of the FLIM system.
- (2) Start the LSC software on the microscope computer, and start the SPCM and DCC software on the FLIM computer.
- (3) Turn on the laser. For D FLIM systems, see Laser Setup for D FLIM, page 12. For multi-photon systems, see Laser Setup for MP FLIM, page 13.
- (4) Set the imaging parameters in the LCS software, see 'Setup of Imaging Parameters in LCS Software, page', page 14. Set the scan speed, the frames size, and the mode and line average parameters. Select a reasonable pinhole size. For D FLIM, start with a pinhole size of 1 AU. For MP FLIM, open the pinhole entirely. Select an appropriate blocking filter, and set the external port ('ExDet') into the '--' position. Start a continuous scan (click on the  button).
- (5) Load a data file of a previous measurement or setup file into the SPCM software. Use a file that corresponds to the type of the laser used, the laser repetition rate, and desired number of pixels and time channels. See 'Loading Setup and Measurement Data', page 28.
- (6) Enable the outputs of the detector controller, and open the shutter, see DCC-100 S, page 18. For the standard PMC-100 detector, set the detector gain to 90 to 100%. Turn on the cooling of the detector. For the PMC-100-0 or -1 detectors moderate cooling (0.6 to 1A, 5V) is sufficient. In extreme cases it may happen that the detector is overloaded and shuts down. In this case, reduce the laser power or the pinhole size and re-activate the detector.
- (7) Adjust the laser power to obtain a CFD and TAC count rate between $50 \cdot 10^3$ and $1 \cdot 10^6$ photons per second. Higher count rates yield better signal to noise ratio for a given acquisition time. However, the high excitation power needed may cause excessive photobleaching. If you have photobleaching you see it by a slow decrease of the count rates.
- (8) If not already running, start a continuous scan in the LCS software (click on the  button). Start the measurement in the FLIM system by clicking on the 'Start' button. Let the measurement run until you are satisfied with the obtained signal-to-noise ratio or until it stops by reaching the specified collection time or number of accumulation cycles. The image you see is either the intensity accumulated over all time channels of the pixels, or the intensity within a selected time gate, see 'Display of Images in the SPCM Software', page 24. Keep in mind that reasonable FLIM in general requires a higher signal-to noise ratio than pure intensity imaging.
- (9) If not stopped yet, stop the measurement by clicking on the 'stop' button. Stop the scan. Save the data by using the 'Save' function of the SPCM software, see page 27. Saving the data into an .sdt file of the SPCM software is important because only these files contain the complete set of photon data and setup data. Only by saving an .sdt file the measurement can be reproduced. After having saved the data, send the measurement to the SPCImage data analysis software.
- (10) Run a data analysis in SPCImage. See 'Data Analysis', page 37.

The steps of recording a FLIM image are summarised on the next page.

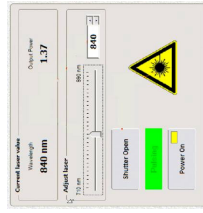
1. Turn on the FLIM system. If you have a lap-top based system, turn on the extension box first, then the laptop computer.



2. Start the DCC-100 and the SPCM application



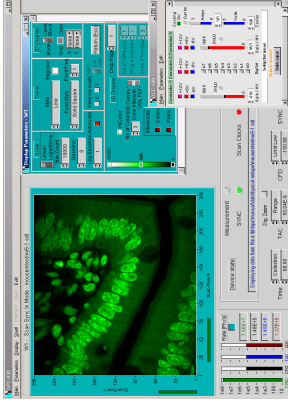
3. D-FIM: Turn on the diode. MF-FLIM: Turn on the MP laser



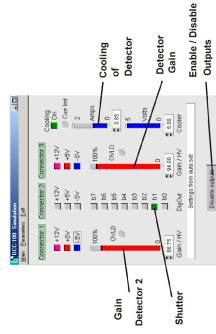
4. Configure the beam path in the TCS SP2 to send the light to the fibre output. Define an image size of 512 x 512 pixels. Start a 'Continuous Scan'.



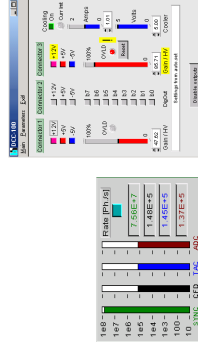
5. Load a setup file, a data file of a successful measurement or use Main, Predefined Setups. Place the DCC panel in a convenient area of screen.



6. Enable the DCC outputs. Open the shutter. Set the detector gain to 90 to 100%. For other parameters use the settings as shown below.

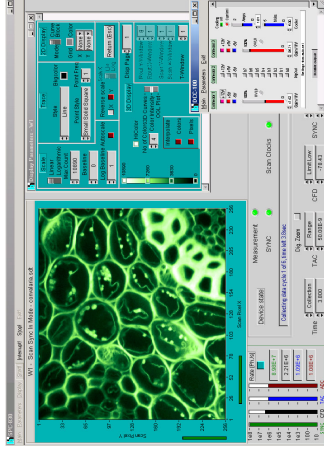


7. Adjust the laser power to obtain a CFD count rate between $5 \cdot 10^4$ and $5 \cdot 10^6$. High power yields higher count rate and shorter acquisition time but may cause increased photobleaching.



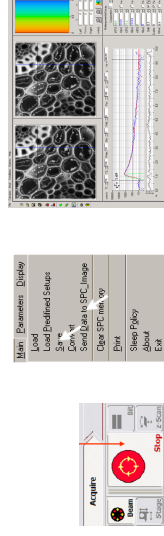
If the detector shuts down by overload (right panel) reduce the laser power or the pinhole size. Then click on the 'Reset' button of the DCC panel to re-activate the detector.

8. Start the measurement in the FLIM system

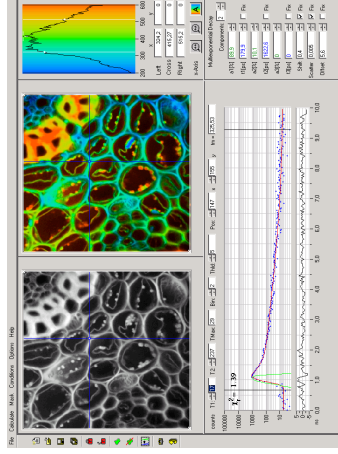


With the pre-defined settings the TCSPC module displays intermediate results in intervals of about 20 seconds. Let the measurement run until you are satisfied by the signal-to-noise ratio.

9. Stop the measurement. Stop the scan in the LCS software. Save the FLIM data by using 'Main', 'Save'. Send the data to the SPCImage lifetime data analysis.



10. Set the cursors as shown in the SPCImage panel. Click on 'Calculate system response', then 'Calculate decay matrix'.



Details of FLIM Data Acquisition

Count Rates

The count rates are displayed in the status window of main panel of the SPCM data acquisition software, see Fig. 32.

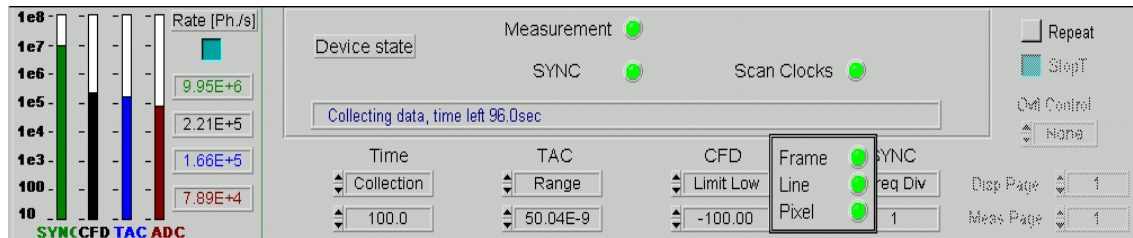


Fig. 32: Count rates (left) status information (upper middle)

The ‘SYNC’ rate is the repetition rate of the laser. For the Ti:Sapphire (multiphoton) laser the SYNC rate must correspond to the specified repetition rate, typically 78 to 92 MHz. A different (usually lower) SYNC rate indicates poor mode-locking. For the diode laser the displayed SYNC rate is lower than the actual repetition rate. The reason is that the laser is switched off during the beam flyback and does not deliver a synchronisation signal during these intervals. This is also the reason that the D FLIM displays a SYNC rate only when the scan is running.

The CFD, TAC and ADC rates indicate the rate of the detected, converted, and stored photons, respectively [19]. The CFD, TAC, and ADC rates are immediate indicators of the progress of a FLIM measurement. The higher the count rate, the faster the photon distribution builds up, and the better the accuracy of the obtained fluorescence lifetimes for a given acquisition time. The count rates may fluctuate due to inhomogeneous intensity in the scan area, due to the beam blanking during the beam flyback, and due to suppression of photons outside the useful scan area.

When a FLIM measurement is running, from time to time take a look at the CFD and TAC count rate. A substantial decrease in the count rates indicates photobleaching. Photobleaching can change the recorded lifetimes. It is not only that different fluorophores or fluorophore in different binding states bleach at different rate, the photobleaching products may also fluoresce themselves. As long as the total decrease in the CFD rate does not exceed 20 % the effect on the lifetimes may still be acceptable. If the drop is larger you either have to reduce the laser power or to increase the detection volume, see below, ‘Photobleaching’.

Both the SPC-830 module and the PMC-100 detector work well up to a detected (CFD) count rate of about 8 MHz. Although there is about 50% loss of photons at a count rate this high systematic errors in the recorded lifetimes are still small [18, 19]. You should, however, take into regard that the displayed count rates are averages over the whole scanning cycle, including the beam flyback. With the sample reasonably filling the image area you can use CFD count rates up to a few million photons per second.

In practice you will reach such count rates only for strongly stained samples of exceptionally high photostability. Except perhaps for a few pH or ion concentration imaging tasks the count rates obtained from typical FLIM samples are considerably lower. The effects investigated by FLIM normally require the fluorophores to be located in highly specific sub-units of the cells. Or, in case of autofluorescence imaging there is no endogenous fluorophore at all. Consequently, the fluorophore concentrations are low, and so are the count rates. The theoretical limit to lower count rates is set by the detector dark count rate. With the PMC-100 detector

you can record lifetime data down to less than 1000 photons per second. Count rates this low do, of course, require long acquisition times.

Photobleaching

As mentioned above typical FLIM samples are characterised by low fluorophore concentration. Moreover, most of the effects investigated by FLIM have to be measured at living samples. The fluorescence intensity of these samples is low. The attempt to obtain high count rates from by increasing the excitation intensity usually results in excessive photobleaching or even photodamage. Both effects can cause noticeably cause changes in the lifetimes [17]. Usually slow lifetime components bleach faster, and the lifetime distribution changes. Moreover, the photobleaching products may be fluorescent themselves.

Photobleaching is clearly nonlinear for two-photon excitation [80], and a nonlinear component probably also exists for one-photon excitation [25]. Therefore, photobleaching can be reduced by decreasing the excitation power and compensating for the lower count rate by an increased acquisition time.

For the D-FLIM you may also increase the pinhole size. The increases detection volume allows you to obtain the same count rate at a lower laser power. A slightly impaired resolution may be better than unpredictable lifetime changes by photobleaching.

It is often believed that photobleaching is lower for two-photon excitation than for one-photon excitation. This is not generally correct. Of course, two-photon excitation does not yield excitation outside the focal plane, and, consequently no photobleaching. However, for the same number of emitted fluorescence photons photobleaching within the scanned plane is stronger [42]. If photobleaching is a problem and your system contains both an MP laser and a diode laser a comparison between both excitation principles may be useful.

Giving general recommendations for adjusting the count rate is difficult. On the one hand, the concentration of the fluorophore and the photostability may vary by orders of magnitude, on the other hand the tolerance of the users to possible artefacts may differ considerably. In published FLIM results the count rates and the amount of photobleaching are rarely mentioned so that only a few examples can be given here. CFP-YFP FRET images of HEK cells presented in [15, 16] were recorded at $50 \cdot 10^3 \text{ s}^{-1}$. CFP-YFP FRET in *Caenorhabditis Elegans* [32] was recorded at $< 10^5 \text{ s}^{-1}$. Two-photon autofluorescence of skin delivered about $60 \cdot 10^3 \text{ s}^{-1}$ [68, 69, 70]. These count rates are by factor of 40 to 100 lower than the maximum recorded count rate of the bh TCSPC devices used. It should be expected that much higher count rates are obtained from stained tissue. However, imaging of the pH in skin tissue by BCECF was performed at an average rate of only $2 \cdot 10^6 \text{ s}^{-1}$ [54], although the frequency-domain technique used was capable of processing much higher rates.

Acquisition Time of FLIM

From a single-exponential fluorescence decay recorded under ideal conditions the fluorescence lifetime can theoretically be obtained with a relative standard deviation or ‘coefficient of variation’, CV_τ , of

$$CV_\tau = \frac{\sigma_\tau}{\tau} = \frac{1}{\sqrt{N}} \quad (1)$$

with N = number of recorded photons [5, 49, 63]. In other words, the fluorescence lifetime can be obtained with the same accuracy as the intensity. Measurement under ideal condition means the decay function is recorded

- with an instrument response function of negligible width
- into a large number of time channels
- over a time interval considerably longer than the decay time
- with negligible background of environment light and detector dark counts or detector afterpulsing

The equation given above can be used to estimate the number of photons and the acquisition time needed to record a fluorescence lifetime image. The relative lifetime accuracy for a given number of photons per pixel is shown in Fig. 33, left. The diagram shows that the standard deviation improves only slowly with the number of photons. A lifetime accuracy of 10 % can ideally be obtained from only 100 photons. However, 10,000 photons are required to obtain a lifetime accuracy of 1 %.

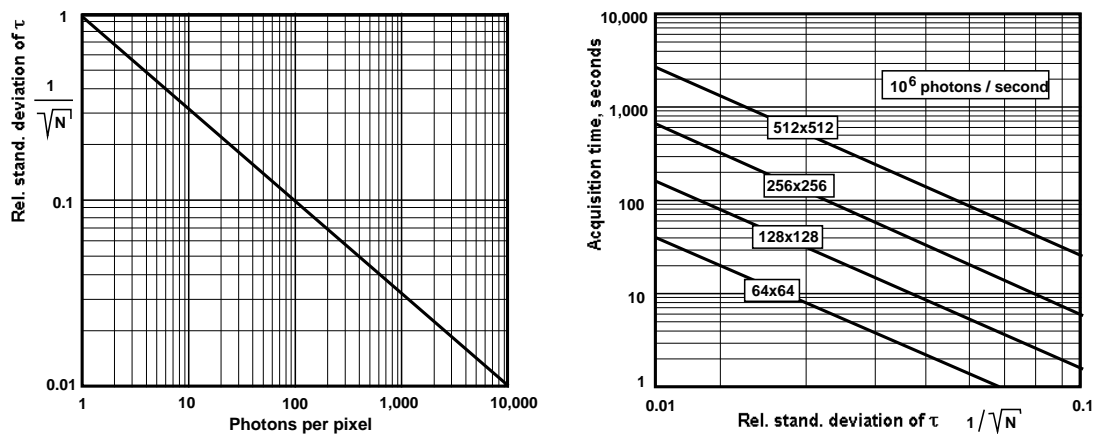


Fig. 33: Left: Relative standard deviation versus the average number of photon per pixel. Right: Acquisition time as a function of the desired lifetime accuracy for different image sizes. Count rate 10^6 s^{-1} .

The acquisition time as a function of the desired standard deviation for a count rate of 10^6 s^{-1} is shown in Fig. 33, right. Even for an image of 512 x 512 pixels a relative lifetime accuracy of 0.1 (or 10%) is obtained within less than 30 seconds, for smaller pixel numbers the acquisition time is correspondingly shorter. However, an acquisition time of almost 1 hour would be required to record lifetime image of 512 x 512 pixels with a lifetime accuracy of 1 %.

The accuracy obtained in practice may differ from the values shown in Fig. 33. In particular, the background count rate in FLIM experiments is often not negligible, and the fluorescence may not decay entirely within the laser pulse period. Moreover, a count rate of 10^6 s^{-1} is a relatively optimistic assumption.

The required number of photons increases if double-exponential decay functions are to be resolved. In [63] the number of photons required to resolve a double-exponential decay is given with $N = 400,000$. A number of photon per pixel this high is, of course, entirely beyond the limits set by the photostability of a biological sample. [63] is therefore often used as an argument that double-exponential lifetime imaging is impossible.

Fortunately, the prospects to separate two lifetime components improve dramatically with the ratio of the two lifetimes and with the amplitude factor of the short lifetime component. The lifetime components assumed in [63] were 10 % of 2 ns and 90 % of 4 ns. This is an extremely unfavourable situation which indeed requires an extremely high number of photons. Fortunately, the decay profiles encountered in FRET and autofluorescence measurements have a much more favourable composition, see Fig. 4, page 4. Usually the lifetime components are separated by a factor of 5 to 10, and the amplitude of the fast component is 50 to 90%. Under such conditions double or even triple exponential analysis is feasible on no more than a few 1000 photons per pixel, and very satisfactory results are obtained from 10,000 photon per pixel. Nevertheless, the required photon numbers are difficult to obtain, especially for image

sizes of 512 x 512 pixels and samples of poor photostability. If the images size cannot be reduced the solution is binning of the lifetime data, see ‘Binning of Pixels in the Data Analysis’, page 42.

It should be noted here that long acquisition time is *not* a feature of FLIM in general or TCSPC FLIM in particular. As shown above, the lifetime accuracy is comparable to the accuracy of intensity images. The difference is that typical TCSPC FLIM applications are aiming at effects not or not fully accessible by steady-state imaging. The lifetime changes caused by these effects are usually small. Consequently, the accuracy requirements (and the expectations) to FLIM results are higher than to steady-state images.

Inexperienced FLIM users often stop the acquisition once they see an intensity image of satisfactory signal-to-noise ratio. The pitfall is, however, that an image with 10 % intensity noise looks very pleasing, while a lifetime accuracy of 10 % is not sufficient for the majority of FLIM applications. Therefore the general advice is: *Run the FLIM acquisition for a time as long and at a count rate as high as the photostability of the sample allows you.*

Image Size

The acquisition time increases linearly with the number of pixels recorded. This statement may be considered trivial. Nevertheless, it is often ignored by microscope users. A laser scanning microscope scans the image area with a constant pixel dwell time, regardless whether or not the pixels contain useful information. Thus, you can decrease the acquisition time by excluding useless pixels from being recorded. The simplest way of achieving this is to zoom into the right area of the image, see Fig. 34.

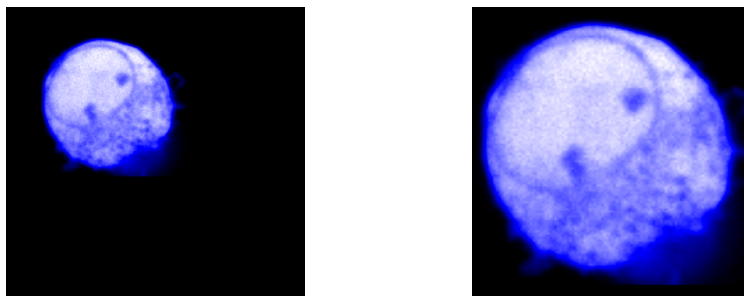


Fig. 34: Image of a single cell. Left: Without zoom; the image contains only 15 % pixels with useful information. Right: After zooming into the correct region of interest 75% of the pixels are used. The acquisition time is reduced by a factor of 5.

The cell shown in the left image fills only 15% of the total scan area. In other words, only 15% of the acquisition time are spent on recording the image of the cell. 85% of the time are spent on recording dark pixels. After zooming into the an appropriate region of interest the cell fills 75% of the scan area, and 75% of the acquisition time are used to image the cell. This is an improvement of a factor of 5 over the recording shown left. You may object that the zoomed image of the cell has also 5 times more pixels, and thus contains the same number of photons per pixels as Fig. 34, left. This is undoubtedly correct. However, with the zoom you may either record the FLIM image with less pixels or use pixel binning in the lifetime analysis (see ‘Binning of Pixels in the Data Analysis’, page 42). You then obtain an image that shows the cell with the same number of pixels as Fig. 34, left, but with a higher number of photons. Binning in the lifetime analysis has the additional benefit that only the lifetimes are binned, not the intensity information.

Data Analysis

Introduction

A measurement in the FLIM mode of the SPC-830 delivers the photon distribution over the coordinates of the scan, the time within the fluorescence decay, and, if several detector in different spectral channels are used, the wavelength, see Fig. 6, page 7. The data can be considered an array of pixels, each containing a large number of time channels spread over the fluorescence decay. In other words, the FLIM measurement delivers images with a decay curve in each pixel, see Fig. 35, left. Several such arrays may exist if several detectors are used.

To obtain fluorescence lifetimes the decay curves in the individual pixels must be fitted with an appropriate model. However, the measurement system is not infinitely fast. Therefore the fitting routine has to take the ‘instrument response function (IRF)’ into account. The IRF is the pulse shape the FLIM system records for an infinitely short fluorescence lifetime. The fitting procedure convolutes the model decay function with the IRF and compares the result with the photon numbers in the subsequent time channels of the current pixel. Then it varies the model parameters until the best fit between the convoluted model function and the measured decay data is obtained.

Typical models are single exponentials or a sum of exponential terms. The models are normally characterised by several parameters, e.g. the fluorescence lifetimes of the exponential terms and their amplitudes. The fitting procedure delivers these parameters for all pixels of the scan (Fig. 35, middle). The pixels of the resulting lifetime data array contain the results of the fitting procedure (Fig. 35, right).

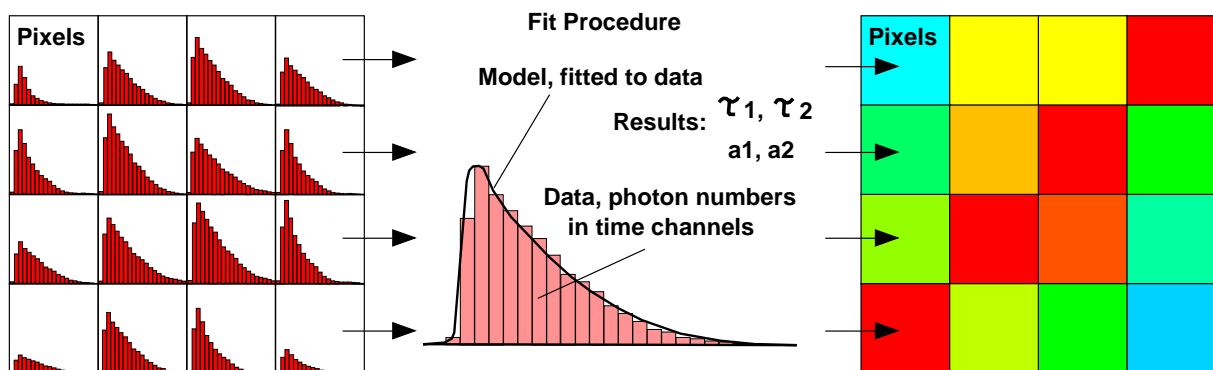


Fig. 35: Analysis of FLIM data. Left: Raw data, pixels contain decay curves. Middle: Fit procedure, delivers lifetimes and amplitudes for individual pixels. Right: Lifetime data: Pixels contain results of fit procedure

In the simplest case, the decay curves of the individual pixels can be characterised by a single-exponential model. The result of the fitting procedure is then a single fluorescence lifetime. Lifetime images created from such data use the number of photons per pixel (the intensity) as brightness and the fluorescence lifetime as colour, see Fig. 36.

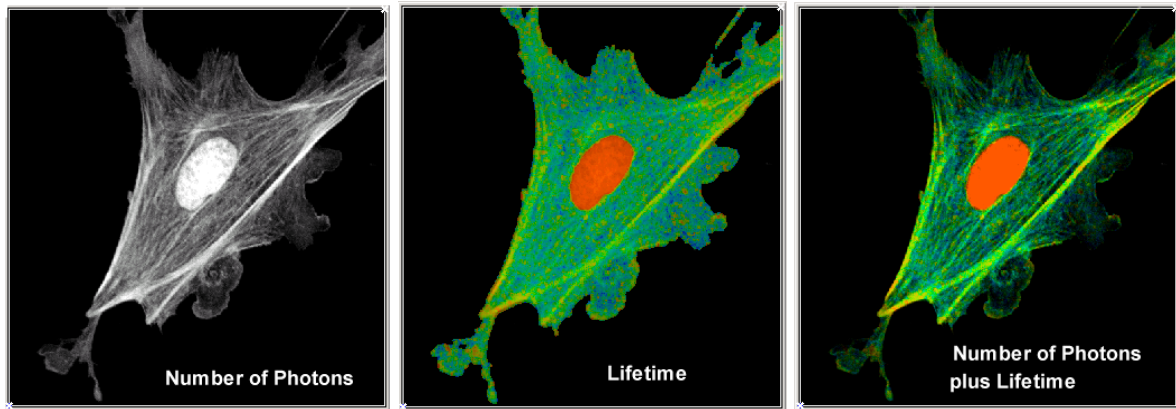


Fig. 36: Combination of the intensity and the lifetime information. Left: Intensity image, brightness represents total number of photons per pixel. Middle: Pure lifetime image, colour represents fluorescence lifetime. Right: Combined image, brightness represents number of photons, colour represents fluorescence lifetime.

Fluorescence decay curves of biological samples often contain fluorescence components of several fluorescing species. The decay curves are then multi-exponential (see Fig. 4, page 4). The fitting procedure delivers lifetimes and amplitude coefficients for the individual exponential components. For example, a double exponential decay function is described by

$$N(t) = a_1 \cdot e^{-t/\tau_1} + a_2 \cdot e^{-t/\tau_2} \quad (a_1 + a_2 = 1) \quad (2)$$

Fitting the decay curves with this model delivers the lifetimes, τ_1 and τ_2 , and the amplitudes, a_1 or a_2 . It is, of course, impossible to display three independent decay parameters and the fluorescence intensity simultaneously in one image. The analysis software therefore provides a number of options for the display of the parameters. You may assign either τ_1 , τ_2 , a_1 or a_2 to the colour of the display, or you may use ratios, such as τ_1 / τ_2 or a_1 / a_2 . An example is given in Fig. 37. It shows the same cell as Fig. 36, but analysed by a double-exponential model.

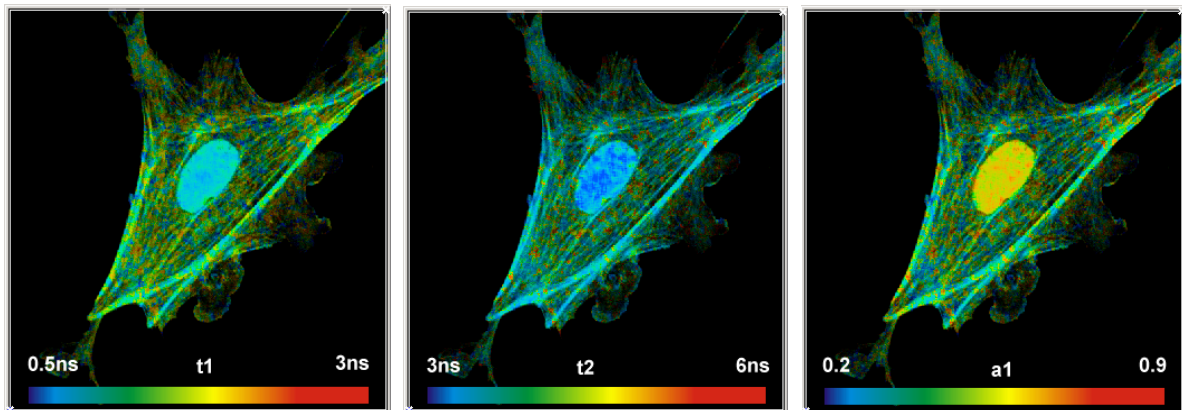


Fig. 37: Double-exponential decay analysis. Left to right: Images showing the decay time of the fast lifetime component, the decay time of the slow lifetime component, and the intensity coefficient of the fast lifetime component.

Frequently used functions of the ‘SPCImage’ FLIM data analysis software are described in the following paragraphs. A comprehensive description is given in [9].

Analysing fluorescence lifetime images

The main panel of the SPCImage data analysis software is shown in Fig. 38. The panel shows an intensity image (upper left), a lifetime image (upper middle), a lifetime distribution over a region of interest (upper right), and the fluorescence decay curve in a selected spot of the image.

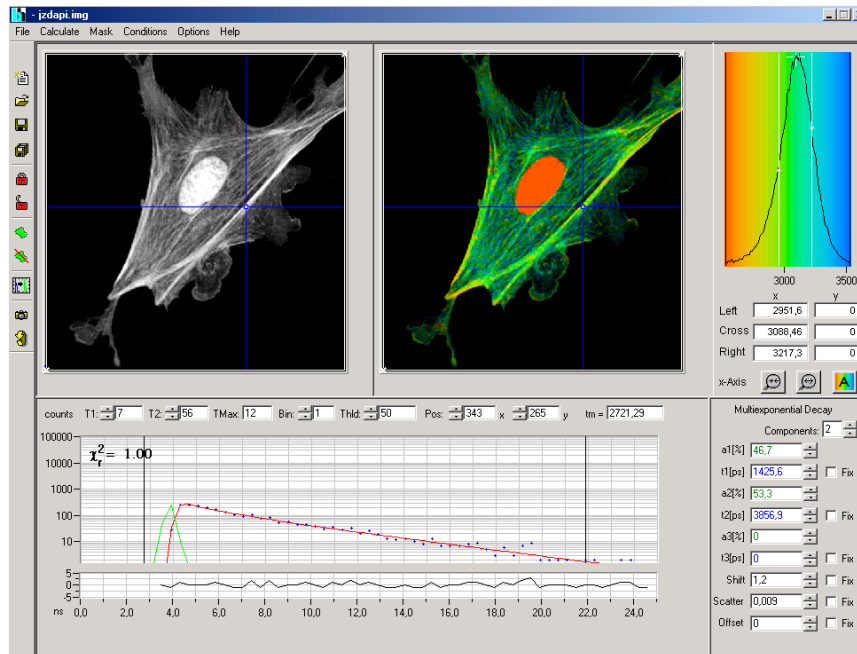


Fig. 38: Main panel of SPCImage

Loading of FLIM Data

There are two ways to load FLIM data into SPCImage, see Fig. 39. You can open SPCImage, and click on 'File', 'Import'. The import routine of SPCImage loads the .sdt files saved by the SPCM data analysis software. The second way to load data is by using the 'Send data to SPCImage' function of the SPCM software. The function automatically opens SPCImage and transfers the data. If several detectors are used SPCM sends the data within the 'Routing Window' of the active display window. If you use this option, please do not forget to save the raw data into .sdt file.

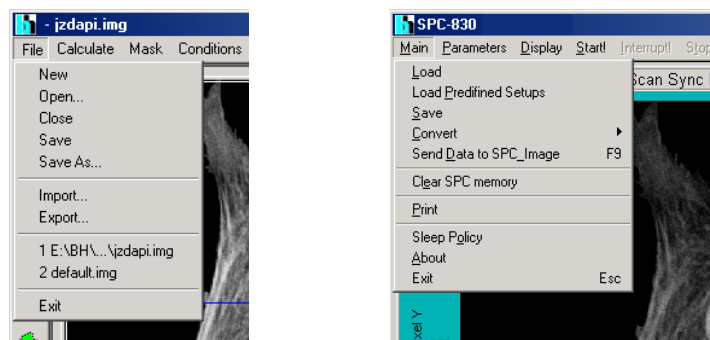


Fig. 39: Loading of FLIM data. Left: Import of an .sdt file via 'File', 'Import'. Right: Sending data directly from the SPCM data acquisition software

Loading the FLIM data via the 'Import' function of SPCImage opens an information and data selection panel, see Fig. 41. For FLIM data recorded by a single detector in a single memory page of the SPCM software there is nothing you can select. Just click on 'OK' and load the

data. However, FLIM data may also be recorded by several detectors, by the bh multi-spectral (MW-FLIM) system [7, 19], or within several memory pages of the SPCM software. For such data you can select a window of routing channels and page numbers. FLIM data may also be recorded in a multi-module TCSPC system [19]. In this case you can select the TCSPC module or a range of TCSPC modules.

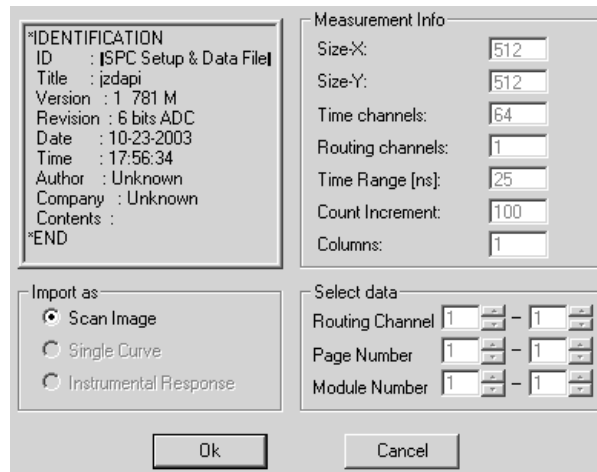


Fig. 40: Information and data selection panel of the SPCImage import function

Hot Spot and Region of Interest Selection

After the FLIM data have been imported SPCImage displays an intensity image of the loaded FLIM data, see Fig. 41.

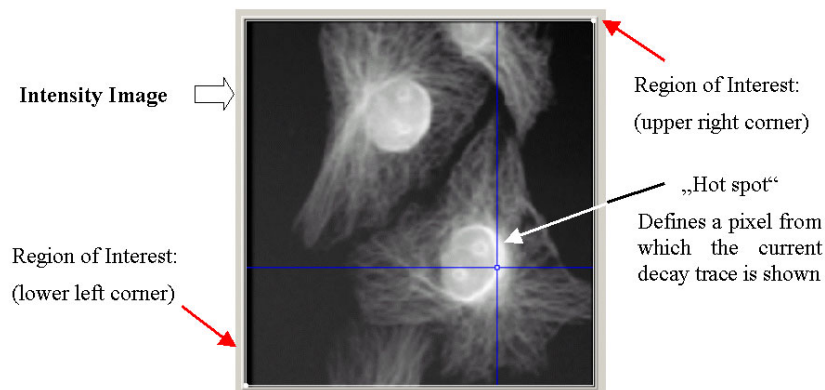


Fig. 41: Intensity image after import of FLIM data

After loading the data the software will choose the brightest pixel of the image as a 'Hot spot'. The location is indicated by the blue crosshair. It is also given as a numerical position (x,y) in the decay window which is described below. The Hot Spot is used to calculate an IRF for the fitting procedure (see below, 'Instrument Response Function'). The same spot is used to display a fluorescence decay curve (see Fig. 43). If necessary, the pixel selection can be changed by moving the blue crosshair.

Two white crosshairs are located in the upper right and lower left corner of the image. They define a region of interest (ROI) which will be used in the data analysis. They can be changed by clicking on the white dots and moving them to a different location. Defining ROIs may save computation time since only the data of the area within the crosshairs are processed.

Instrument Response Function

Measuring the IRF requires to record the laser pulses through the normal optical path of the detection system. In microscopes this is difficult because the same beam path is used for the excitation and emission light. The laser light is scattered at many optical surfaces inside the microscope, and a clean reflection from the sample plane is usually not obtained. In multi-photon microscopes second harmonic generation or hyper-Raman scattering can be used [53], but even then IRF recording is not easy.

The SPCImage data analysis software therefore estimates an IRF from the recorded data. The instrument response function can either be calculated automatically or on command. The decision is made under 'Options', 'Preferences', see Fig. 42. Calculation on command is started by clicking into 'Calculation', 'System Response'.

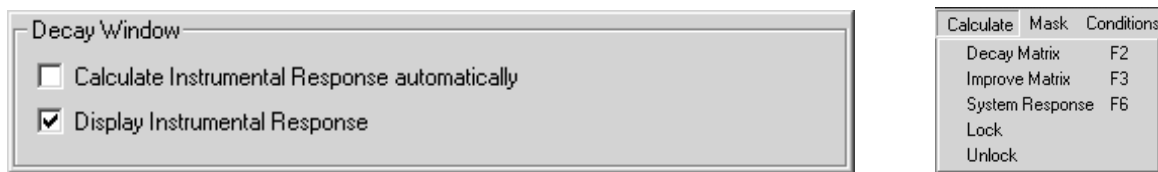


Fig. 42: Definition of the calculation and the display of the IRF (left) and calculation of the IRF on command (right)

Unless you tend to forget to start the IRF calculation we recommend *not* to use the automatic calculation. Calculation on command gives you the chance to select the best location in the image and the best binning factor. In any case, you should switch on 'Display Instrumental Response' to make sure that your data analysis is based on a reasonable IRF.

Fit Selection Parameters

The decay curve in the 'Hot Spot' of the image is displayed beneath the intensity image, see Fig. 43. It shows the photon decay data in the subsequent time channels of the selected pixel (blue), the convolution of the model function and the IRF fitted to the decay data (red) and the response function (green). The deviations between the photon data and the fit-trace are shown at the bottom. The values shown are weighted residuals.

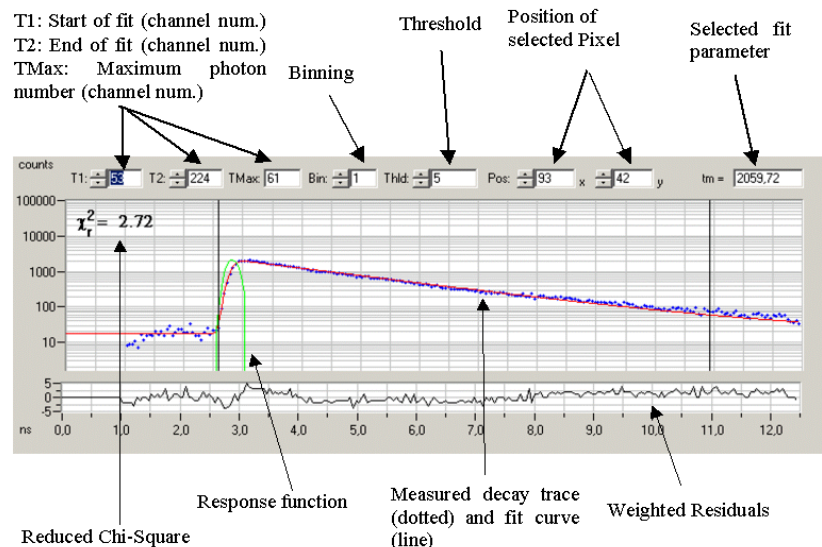


Fig. 43: Decay curve window

The time interval in which the fitting is done is selected by two vertical cursor lines. The cursor positions, T1 and T2, are shown numerically in the status line above the decay curve win-

dow. The setting of the cursors have considerable influence on the fit quality. The left cursor should be set at the beginning of the rise of the fluorescence curve or a few time channels left of it. However, a few time channels should remain left of the left cursor. These channels are used to calculate the baseline offset. The right cursor should be set at the last reasonable time channel of the fluorescence decay curve. There may be a few time channels at the right end of the curve that drop visibly below the expected level of the curve. The drop results from the ADC error correction technique used in the SPC-830 module [18, 19]; the channels should therefore be excluded from the fitting.

Parameters frequently used to control the fit procedure are displayed above the decay curve window:

- *T1 and T2* are the positions of the cursors in the decay curve window. Only the data points between the cursors are used for the fit.
- *TMax* is the time channel in which the fluorescence is at maximum.
- *Binning* defines an area around the current pixel the photon data of which are combined for lifetime analysis. The binning factor is adjusted according the number of photons in the raw data, the spatial oversampling factor used when the image was recorded, and the complexity of the decay model used. Please see below, ‘Binning of Pixels in the Data Analysis’.
- *Threshold* defines a minimum number of photons in the peak of a fluorescence curve. Pixels with lower photon numbers are not analysed by the fitting procedure. ‘Threshold’ is used to suppress dark pixels. This not only accelerates the calculation process but also improves the quality of the lifetime parameter histogram (see ‘Lifetime Parameter Histogram’, page 48).
- *Pos. X and Y* shows the position of the blue crosshair in the intensity and the lifetime image.
- The field far right shows the fluorescence lifetime in the ‘hot spot’ or in the pixel selected by the blue crosshair. Default is the mean lifetime, τ_m , defined by

$$\tau_m = \frac{\sum_{i=1}^N a_i \tau_i}{\sum_{i=1}^N a_i} \quad (3)$$

For a single exponential decay τ_m is identical with the fluorescence lifetime, τ . Please note that τ_m of a multi-exponential fit is not identical with the lifetime obtained from a single-exponential fit of the same data.

Binning of Pixels in the Data Analysis

When an image is taken by a scanning microscope the point-spread function of the microscope lens is usually ‘oversampled’ to obtain best spatial resolution. As a rule of thumb, the diameter of the central part of the Airy disc should be sampled by 5×5 pixels, see Fig. 44, left. In practice even higher oversampling factors are often used unintentionally. Under these conditions lifetime data should be calculated from several binned pixels. When the binning function of SPCImage is used the lifetime images are built up from the unbinned intensity pixels and the binned lifetime pixels. This yields substantially improved lifetime accuracy without noticeable loss in spatial resolution. Sampling artefacts are largely avoided by overlapping binning, see Fig. 44, right.

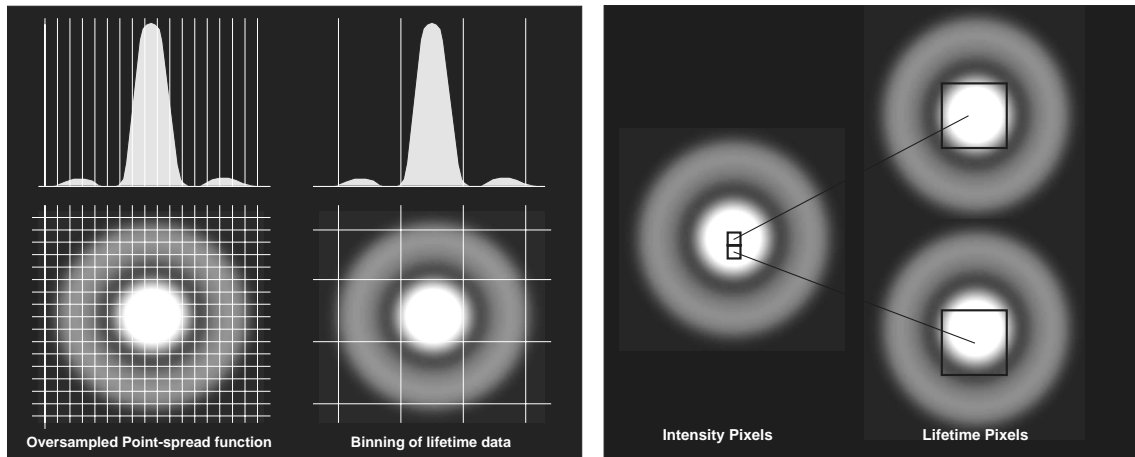


Fig. 44: Left: Oversampling of the Airy disc in the intensity image and binned pixels for lifetime calculation. Right: Overlapping binning of pixels for lifetime calculation.

The binning is controlled by the 'Bin' parameter above the decay curve window. The function of the parameter is shown in Fig. 45. 'Bin' defines the number of pixels around the current pixel position. Please note that the number of pixels of the lifetime image is not reduced. Only the lifetimes are calculated from the combined pixels, the intensities remain unbinned.

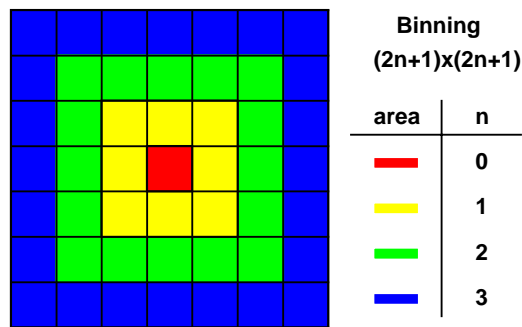


Fig. 45: Function of the binning parameter

Fig. 46 shows lifetime images obtained from a 512 x 512 pixel scan. The binning was set to 1, 4, and 6 (left to right). As can be seen from these images there is little loss in detail even at large binning factors.

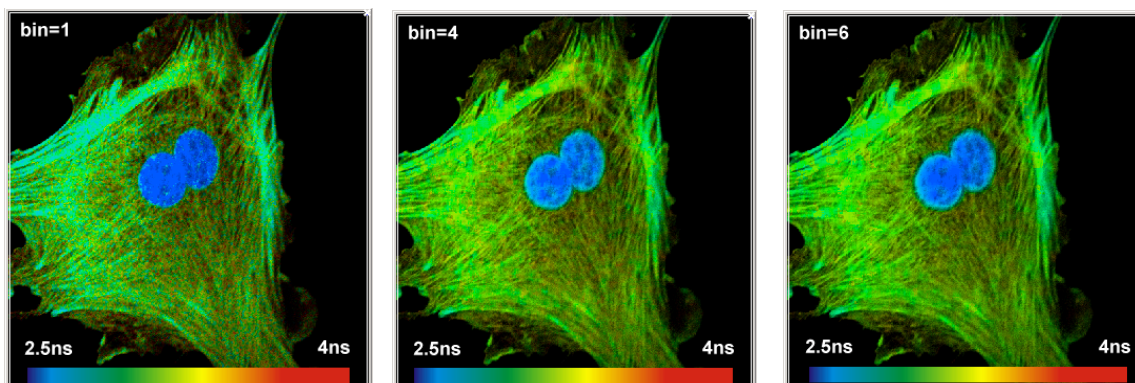


Fig. 46: Lifetime images obtained from a 512 x 512 pixel scan. Left to right: Binning 1, 4, and 6

Model Selection

The model parameters are selected in a panel right of the decay curve window, see Fig. 47.

- Components: Number of exponential components used by the model
- t1, t2, t3: Lifetimes of the exponential components
- a1, a2, a3: Amplitudes of the exponential components
- Shift: Shift between the calculated or loaded IRF and the actually used IRF.
- Scatter: Amount of scattered excitation light detected, or amount of other ‘prompt’ emission. Can be used to extract second harmonic generation.
- Offset: Baseline offset of the decay curve. Offset is not really a fitting parameter. its is determined from the time channels left of the left cursor, see Fig. 43.

Multiexponential Decay		
Components:	2	
a1[%]	39	
t1[ps]	694,3	<input type="checkbox"/> Fix
a2[%]	61	
t2[ps]	2558,8	<input type="checkbox"/> Fix
a3[%]	0	
t3[ps]	0	<input type="checkbox"/> Fix
Shift	1,0	<input type="checkbox"/> Fix
Scatter	0,019	<input type="checkbox"/> Fix
Offset	14	<input type="checkbox"/> Fix

Fig. 47: Model selection parameters

More model parameters are available under ‘Options’, ‘Model’. The corresponding panel is shown in Fig. 48

Fit Model	
<input checked="" type="radio"/> Multiexponential Decay	Repetition Time: 0,000 ns
<input type="radio"/> Incomplete Multiexponentials	
Parameter Constraints	
Minimum Lifetime:	100 ps
Maximum Lifetime:	30000 ps
Minimum Ratio	1
Algorithmic Settings	
Iterations (max):	10
Delta Chi ² (min):	0,010
<input type="checkbox"/> Allow negative amplitudes	
Offset-Correction	
<input type="checkbox"/> Manual Selection	First: 0 Last: 34

Fig. 48: Model parameter options

- Multi-exponential decay: The model is a sum of exponential terms.
- Incomplete multi-exponentials: The model is a sum of exponential terms. It takes into account that the fluorescence does not fully decay within a single laser pulse period. Based on ‘Repetition Time’ the fluorescence left over from all previous excitation pulses is included in the model.
- Repetition Time: Time between the laser pulse for ‘Incomplete multi-exponentials’.
- Parameter constraints: Minimum lifetime, maximum lifetime, and minimum ratio of the lifetimes of two exponential terms used to fit the data.
- Algorithmic Settings: Maximum number of iterations and minimum difference in the χ^2 between subsequent iterations. Negative amplitudes of lifetime components may or may not be allowed for. Negative amplitudes may occur in the fluorescence decay of the acceptor of a FRET system, in the fluorescence of excimers, and in fluorescence depolarisation measurements.

Which Model Should I Use?

It is often not clear which model, in particular which number of exponential components, should be used to fit the data. If there is no a priori knowledge about the shape of the fluorescence decay the model can only be found by try and error.

It is normally not difficult to find the appropriate number of exponential components. Select a characteristic spot of the sample. Increase the binning factor until you see a clear fluorescence decay function. Then change the number of components and check the displayed χ^2 and the curve of the residuals. A good fit is characterised by a χ^2 close to one, and residuals showing no noticeable systematic deviations. Often you see a poor fit already by comparing the fitted curve (red) with the photon data (blue) in the decay window.

In most cases your decay curves will be fitted adequately by a single- or double-exponential model. If you define more exponential components than needed to fit the data you normally get two components of almost identical lifetime, or an extremely long lifetime component of very low amplitude. An example is shown in Fig. 49.

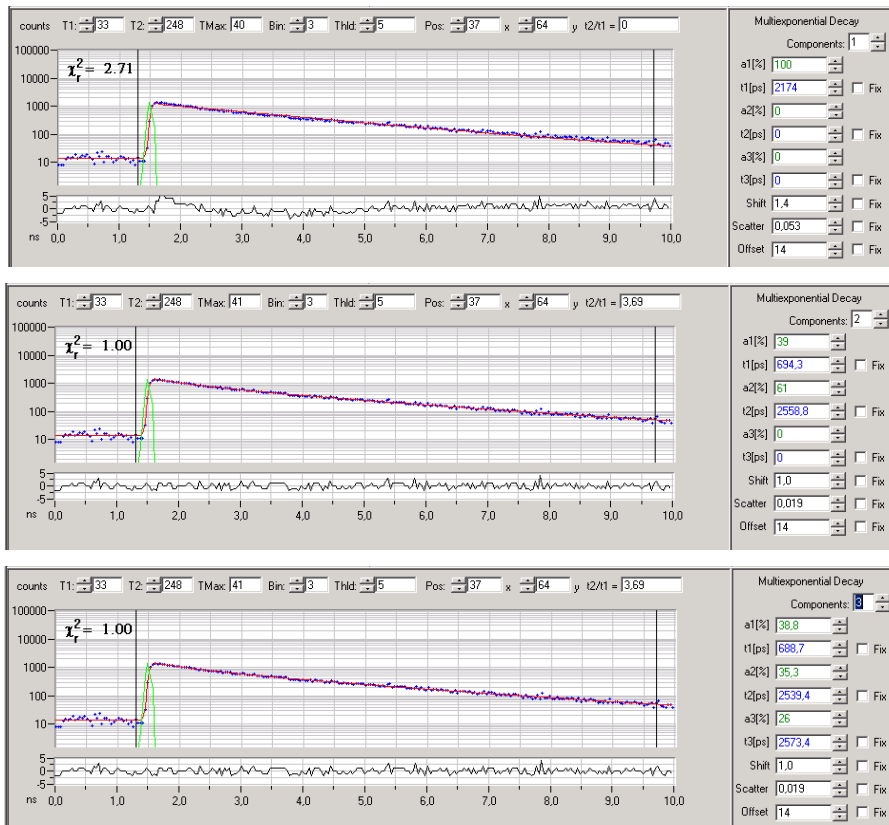


Fig. 49: To bottom. Fitting a decay profile with one, two, and three exponential components

Fitting the data with only one component (Fig. 49, top) delivers a large χ^2 and clearly visible systematic variation in the residuals. With some experience, you may also spot systematic deviations between the decay data and the red curve calculated by the fitting procedure.

Fitting the data with two components delivers a perfect χ^2 and removes any systematic variations in the residuals. This is an indication that the fit cannot be improved by adding more exponential components.

A attempt to fit the data with three components (Fig. 49, bottom) indeed does not yield any improvement. Instead, it delivers a third lifetime component almost identical with the second one. This is a clear indication that the double-exponential model is the right one.

Deriving an ‘Apparent’ Lifetime from a Multi-Exponential Decay

Sometimes the fluorescence decay functions are clearly multi-exponential, but only the lifetime of a single-exponential approximation is needed. A typical example is FRET measurements and pH measurements. The FRET donor decay functions normally show the decay components of interacting and non-interacting donor molecules. For calculating distances

these components must be resolved. However, if the task is only to determine where FRET occurs in a cell single-exponential analysis is sufficient. In pH measurements usually the lifetimes of a protonated and a deprotonated form of the fluorophore are discernible, but the pH can better be determined from a single-exponential approximation. In these cases, do not hesitate to use a single-exponential fit, even if it delivers a large χ^2 . Because the number of model parameters is smaller (see below) the lifetime accuracy may be better than for an average or mean lifetime calculated from a double-exponential fit.

Which Model Parameters Should I Use?

In general, the accuracy of a fit procedure is the better the lower the number of model parameters is. In particular, the fitting routine has a hard time to determine parameters which have an almost identical influence on the modelled curves. These may be

- the shift parameter and an extremely short lifetime component
- the scatter and an extremely short lifetime component
- the offset and a slow lifetime component
- two components with lifetimes close together

Therefore most of the parameters can be set to fixed values. They remain then unchanged during the fitting process. Especially the shift and the scatter can often be fixed, either to zero or to values close to zero. To find the best values, do some tries with large binning in different spots of the image. If you find that the scatter and the shift remain constant, fix them to the indicated values. Fixing the offset is normally not recommended. The offset contains a signal-dependent component caused by the detector afterpulsing. Thus, the offset can only be fixed for detectors of low afterpulsing (MCP-PMTs) and for samples with small relative variation in the pixel intensities.

You may also fix one of the lifetime components. A typical example is the donor fluorescence in FRET experiments. Theoretically, the slow lifetime component comes from non-interacting donor molecules. In first approximation, it should therefore be constant throughout the image. You should, however, be very careful when you use such a priori information. For all decay components there are usually subtle lifetime variations, induced by variation in the local environment or the refractive index [20, 98]. If the lifetime you fixed is not really constant the fitting procedure attempts to compensate for the variations by changing the lifetimes of other components. This can result in large systematic errors.

Calculation of the Lifetime Image

The calculation of the lifetime data is started by clicking into 'Calculate', 'Decay matrix', see Fig. 50.

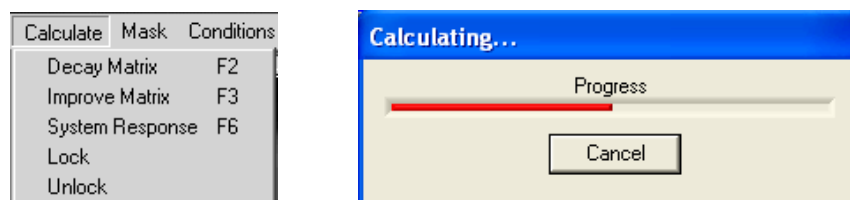


Fig. 50: Calculation of the lifetime image

Especially for double and triple exponential decay models, large pixel numbers, and for large binning factors the calculation can take several minutes. If the calculation is extraordinarily slow we recommend:

- Check the 'Sleep Policy' of the SPCM software. (Click into Main, Sleep Policy). The setting should be 'Never be put to sleep during measurement' and 'Be put to sleep for a longer period outside measurement'.
- Check whether your image contains large dark areas. Set the 'threshold' appropriately to exclude these areas from calculation
- You may also set a 'Region of Interest' to calculate lifetime data only in the area where you really need them.

Display of Lifetime Images

The display of the lifetime image is controlled by the parameters in the 'Colour' and 'Intensity' panel. The panels are shown in Fig. 51.

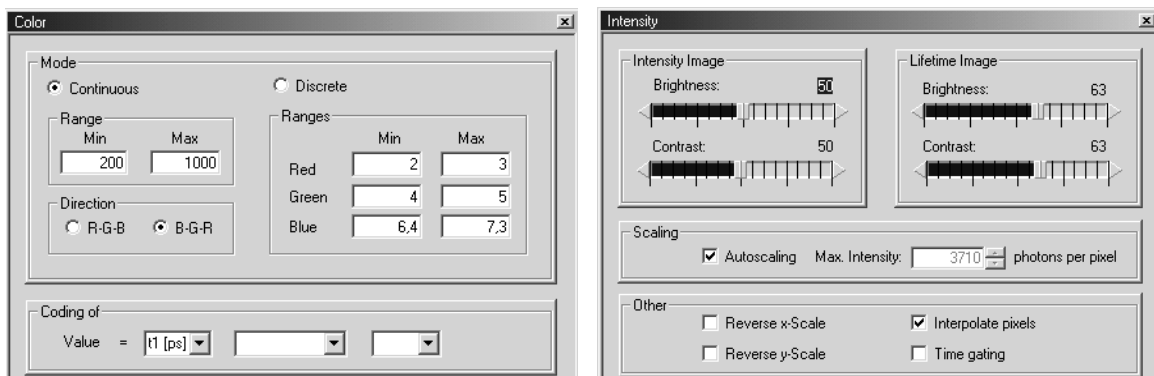




Fig. 51: Control of the lifetime image display. Left 'Colour' panel, right 'Intensity' panel

Please note that the colour and intensity parameters influence only the *display* of the data obtained in the previous lifetime analysis. Thus, you can change the parameters without re-analysing the FLIM data.

- Mode: 'Continuous' defines a continuous colour scale over the specified parameter range. 'Discrete' allows you to assign red, green and blue colour to specified ranges of the parameter displayed.
- Range: Parameter range of 'continuous' colour scale. The colours are assigned to the parameter selected under 'Coding of'
- Direction: The direction of the colour scale can be red-green-blue or blue-green-red.
- Coding of: The colours of the image can be assigned to any of the decay parameters obtained in a single, double, or triple-exponential fit. Moreover, arithmetic expressions of two parameters can be defined.
- Brightness and Contrast: The sliders change the brightness and contrast of the intensity image and the lifetime image.
- Scaling: Assigns the brightness scale to the photon number defined in the 'photons per pixel' field. 'Autoscaling' sets the scale automatically.
- Reverse X scale, Reverse Y scale: The parameters reverse the images in X and Y.
- Interpolate pixels: For images of small pixel numbers the colour and brightness is interpolated between the individual pixels. We recommend to switch 'Interpolate' on to avoid aliasing of the scan pixels with the pixels of the screen.
- Time gating: Normally the intensity is taken from all time channels of the FLIM data. With 'Time Gating' switched on the intensity is taken from the range defined by the cursors in the decay window. Time gating can be useful to exaggerate image details emitting a fast lifetime component on a background of a slow component, or vice versa.

Lifetime Parameter Histogram

SPCImage shows a histogram of the displayed decay parameter calculated over the whole image or over a region of interest, see Fig. 52, left. The parameter may be the lifetime of a fluorescence component, an amplitude factor, or another parameter obtained in the fitting procedure. Depending on the settings in 'Preferences' the histogram either displays the pure pixel frequency or the pixel frequency weighted with the pixel intensities, see Fig. 52, right. The histogram window has two (black) cursors that can be used to select a lifetime interval. The selected interval automatically changes the parameter range of the lifetime image, and vice versa.

 zooms the distribution into the selected parameter range,  zooms out.

 sets the parameter range automatically.

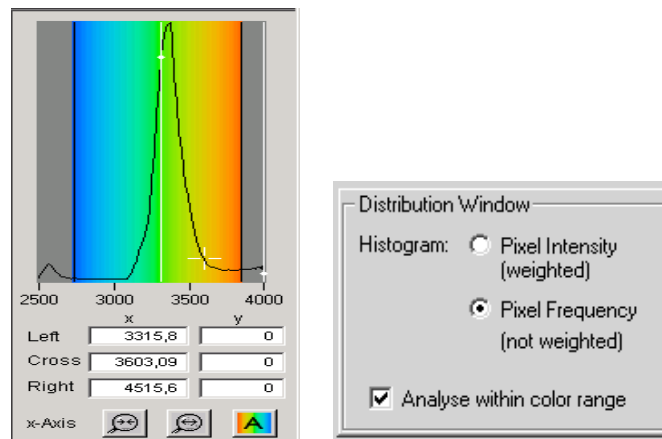


Fig. 52: Lifetime distribution window (left) and definitions in 'Preferences' (right)

Special Commands

For more detailed analysis some additional commands were added to the menu which are available by clicking on the icons in the task-bar.

Calculate → Lock



The Calculate>Lock command should be used if individual data points are analysed after the calculation of the decay matrix. In the "locked" mode no recalculation is performed if the user moves the blue crosshair to different pixels of the image. This guarantees that the colour coding from the last calculation of the decay matrix is consistent with the fitting parameters given for the selected pixel.

Calculate → Unlock



After changing any parameter which may effect the result of the fitting process the matrix have to be recalculated. If the calculation was "locked" by a previous action please use the "unlock" command in order to take the changes into effect.

Polygon definition



The function allows you to define a polygon in which the parameter distribution is calculated. Switch on 'Show Mask Polygon' in 'Preferences' when you use the function.

IRF definition



Defines the curve currently displayed in the decay window as an IRF.

Conditions → Store

After the selection of the fit-model, the time-range for the fitting procedure, the region of interest in the image etc. it is possible to backup all these settings by using the Conditions>Store command. This is especially useful if two images or traces (i.e. acquired in different routing channels) have to be analysed with exactly the same settings.

Conditions → Load

Loads all settings which were saved with the Conditions-Store command.

Special FLIM System Configurations

The bh FLIM systems are modular, and a large number of system configurations are available. Different types of detectors may be used, or several detectors may be operated simultaneously, to detect in several wavelength intervals or under different angles of polarisation. In multiphoton systems, the detectors may be attached to the confocal X1 port, or direct detection via the RLD port may be used. RLD detection systems may even use the bh MW FLIM multi-wavelength detection system. Most FLIM systems use a single TCSPC channel. However, for high-count rate applications systems with several parallel TCSPC channels are available. These non-standard configurations are briefly described below. If you feel you need one of these options, please contact bh. bh and Leica will be happy to work out a solution for your microscope.

Detectors for Multiphoton Direct Detection FLIM

Different detectors available for the multiphoton direct-detection FLIM systems are shown in Fig. 53. Direct detection requires an RLD port adapter to be installed at the microscope. All detectors are connected to the RLD port via a shutter assembly. All FLIM detectors are controlled via the DCC-100 detector controller card of the standard SP2/SP5 FLIM systems.



Fig. 53: Detectors of the bh non-descanned FLIM systems. Left to right: R3809U MCP PMT, PMC-100, H7422P-40, bh MW-FLIM detector

R3809U

The R3809U detector [55] is the detector for ultimate time resolution. Its instrument response function (IRF) has a width of 30 ps (FWHM) [19, 55]. The R3809U is used when lifetimes or lifetime components shorter than 150 ps are to be resolved. Typical applications are FRET experiments with resolution of the interacting and non-interacting donor fraction, tissue auto-fluorescence, and fluorescence of dyes attached to metallic nanoparticles [18]. The maximum continuous count rate of the R3809U is about $1 \cdot 10^6$ photons per second¹. Although this is enough for the majority of applications it should be noted that the R3809U is *not* the right solution to fast-acquisition FLIM.

PMC-100

The bh PMC-100 detector [19] is the standard detector of the Leica FLIM systems. It delivers an IFR of 150 ps FWHM. Lifetimes down to about 100 ps are resolved. The PMC-100 can be used up to the highest count rates applicable with the bh TCSPC boards, without noticeable degradation in the IRF [19]. Typical applications are pH imaging, oxygen imaging, and ion concentration measurements via fluorescence quenching. The PMC-100 works well also for single-exponential FRET measurements, i.e. experiments that do not require separation of the interacting and non-interaction donor fraction. In double-exponential FRET measurements the

¹ The R3809U can be used at count rates up to 3 MHz [18, 19]. However, the output current at this count rate is beyond the permissible maximum specified by Hamamatsu. In FLIM applications high count rates normally occur only in a few pixels of the image. Immediate damage under these conditions appears unlikely; nevertheless life cannot be guaranteed.

longer IRF makes the data analysis more difficult and less accurate than for the R3809U. Autofluorescence imaging is possible as well, though with some compromise in resolution for the shortest lifetime components.

H7422P-40

The H7422P-40 detector [56] has an exceptionally high quantum efficiency. It is recommended for applications that require ultimate sensitivity. In the wavelength range of 500 to 600 nm a sensitivity improvement of a factor of 2 to 3 over the R3809U and the PMC-100 is obtained. The IRF width of the H7422P-40 is 250 to 350 ps. The large IRF width makes the H7422P-40 less useful for FRET and autofluorescence imaging.

Multiphoton Multi-Wavelength FLIM

The MW FLIM detection system [7] detects the fluorescence simultaneously in 16 wavelength channels. As the other direct detection assemblies, the MW FLIM system requires the RLD port to be installed. The fluorescence light leaving the back aperture of the microscope objective lens is projected at the input of a fibre bundle. The fibre bundle transfers this light into the input slit of a polychromator. Fig. 54, left, shows the input of the polychromator with the holder of the fibre bundle. The fibre bundle is shown in the middle. Fig. 54, right, shows the shutter assembly. The shutter assembly contains also the projection lens and a laser blocking filter. The polychromator splits the light spectrally and projects the spectrum on the photocathode of a PML-16 detector. This detector contains a 16 channel PMT and the associated routing electronics. Thus, 16 lifetime images are recorded in a single SPC-810 TCSPC module. Typical applications of the MW-FLIM detector are FRET experiments [30] and autofluorescence imaging [19].

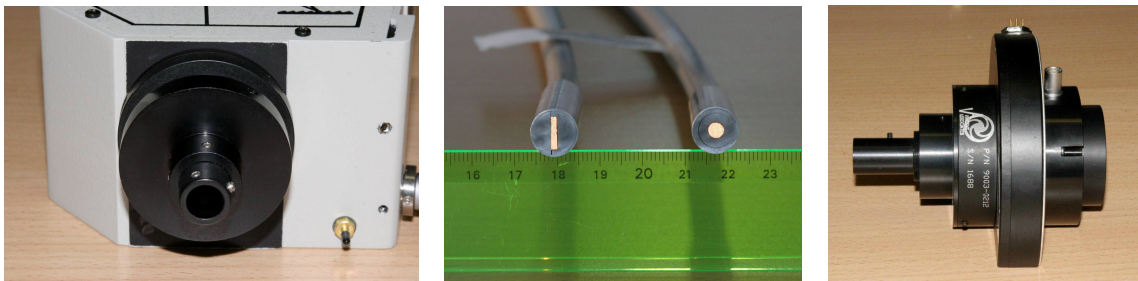


Fig. 54: Details of the NDD MW-FLIM system. Left: Polychromator with adapter for fibre bundle. Middle: Fibre bundle, polychromator end and shutter end, Right: Shutter assembly

Detectors for Confocal FLIM

R3809U

The R3809U detector [55] can also be attached to the X1 port. However, if the R3809U is used in one-photon excitation systems the pulse width of the diode laser limits the resolution. The effective IRF is about 75 ps. In other words, the gain in time resolution over the standard PMC-100 detector is only a factor of two. It appears questionable whether this justifies the considerably higher price of the R3809U. Moreover, the maximum continuous count rate of the R3809U is about $1 \cdot 10^6$ photons per second. Although this is enough for the majority of applications it should be noted that the R3809U is not a solution to fast-acquisition FLIM.

H7422P-40

The H7422P-40 detector [56] has an exceptionally high quantum efficiency. It can be attached to the X1 port. As described for direct detection, the H7422P-40 is used for applications that require ultimate sensitivity. In the wavelength range of 500 to 600 nm a sensitivity improve-

ment of a factor of 2 to 3 over the R3809U and the PMC-100 is obtained. The large IRF width [19] makes the H7422P-40 less useful for FRET and autofluorescence imaging. The H7422P-40 has, however, been used for combined fluorescence correlation (FCS) and fluorescence lifetime measurements. The TCSPC system parameter setup for FCS measurement is described in [19].

MW-FLIM

The MW FLIM detection system [7] can, in principle, also be used in a confocal system. With a suitable adapter, the fibre bundle of the MW FLIM system can be directly connected to the X1 port.

Dual-Detector Systems

For all detectors described above beamsplitter assemblies are available from bh, see Fig. 55, left. Both dichroic and polarising beamsplitters can be inserted. The two detectors are connected to the TCSPC module via an HRT41 router, see Fig. 55, right.

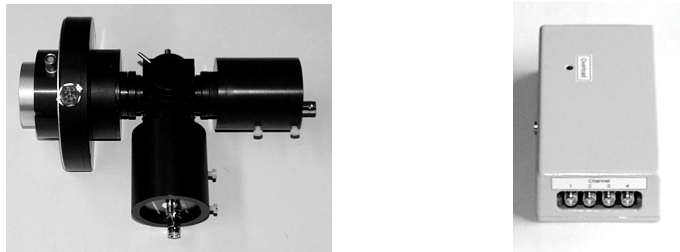


Fig. 55. Left: Beamsplitter assembly with two R3809U detectors. With shutter, configuration for RLD port.
Right: HRT41 router to connect both detectors to one TCSPC module.

Applications

Measurement of Local Environment Parameters

Microscopic pH imaging can be achieved by staining the skin with a pH-sensitive fluorescent probe. These probes usually have a protonated and a deprotonated form. There is an equilibrium between both forms that depends on the pH of the local environment. If both forms have different fluorescence lifetimes the average lifetime is a direct indicator of the pH [73]. A typical representative of the pH-sensitive dyes is 2',7'-bis-(2-carboxyethyl)-5-(and-6)-carboxyfluorescein (BCECF) [57]. In aqueous solution the lifetimes of the protonated form and the deprotonated form have been found 2.75 ns and 3.90 ns, respectively [54]. In the pH range from 4.5 to 8.5 both forms exist, and the fluorescence decay function is a mixture of both decay components. Thus, the lifetime of a single-exponential fit can be used as an indicator of the pH.

The measurement of the concentration of intracellular Cl^- in neurones by TCSPC FLIM was described in [60]. MQAE was used as a fluorescent probe. MQAE is quenched by Cl^- , and the concentration can be calculated from the lifetime change via the Stern-Volmer relation. Because 2-photon excitation does not cause photobleaching and photodamage outside the focal plane the authors were able to obtain z-stacks of the Cl^- concentration in dendrites over depth intervals up to 150 μm .

Fluorescence Resonance Energy Transfer (FRET)

FRET is an interaction of two fluorophore molecules with the emission band of one dye overlapping the absorption band of the other, see 'FRET', page 3. In this case the energy from the first dye, the donor, can be transferred immediately to the second one, the acceptor. The energy transfer itself does not involve any light emission and absorption [47, 73]. Förster resonance energy transfer, or resonance energy transfer (RET), are synonyms of the same effect. The energy transfer rate from the donor to the acceptor decreases with the sixth power of the distance. Therefore it is noticeable only at distances shorter than 10 nm [73]. FRET results in an extremely efficient quenching of the donor fluorescence and, consequently, decrease of the donor lifetime.

Because of its dependence on the distance FRET has become an important tool of cell biology. Different proteins are labelled with the donor and the acceptor; FRET is then used to verify whether labelled proteins are physically linked and to determine distances on the nm scale.

The problem of steady-state FRET techniques is that the concentration of the donor and the acceptor changes throughout the sample, and that the donor and acceptor fluorescence cannot be completely separated spectrally. Steady-state FRET techniques therefore require careful calibration, including measurements of samples containing only the donor or the acceptor. The calibration problems can partially be solved by the acceptor photobleaching technique. An image of the donor is taken, then the acceptor is destroyed by photobleaching, and another donor image is taken. The increase of the donor intensity is an indicator of FRET. The drawback is that this technique is destructive, and that it is difficult to use in living cells.

The use of FLIM for FRET has the obvious benefit that the FRET intensity is obtained from a single lifetime image of the donor. No reference images or calibration measurements are necessary [11, 12, 15, 16, 29, 38, 39, 43].

Single-exponential lifetime images are useful to locate the areas in a cell where the labelled proteins interact. They do, however, not solve the general problem of the FRET techniques that the total decrease of the donor fluorescence intensity or fluorescence lifetime depends both on the distance of donor and acceptor and the fraction of interacting donor molecules. In the simplest case, a fraction of the donor molecules may not be linked to their targets, or not all of the acceptor targets may be labelled with an acceptor. This can happen especially in specimens with conventional antibody labelling [71]. But even if the labelling is complete by far not all of the labelled proteins in a cell are interacting, and the fraction of interacting protein pairs varies throughout the cell.

TCSPC FLIM solves this problem by double-exponential lifetime analysis. The resulting donor decay functions can be approximated by a double exponential model, with a slow lifetime component from non-interacting (unquenched) and a fast component from the interacting (quenched) donor molecules [1, 2, 3, 15, 29, 43, 84, 85]. If the labelling is complete, as it can be expected if the cell is expressing fusion proteins of the GFPs, the decay components directly represent the fractions of interacting and non-interacting proteins. The composition of the donor decay function is illustrated in Fig. 56.

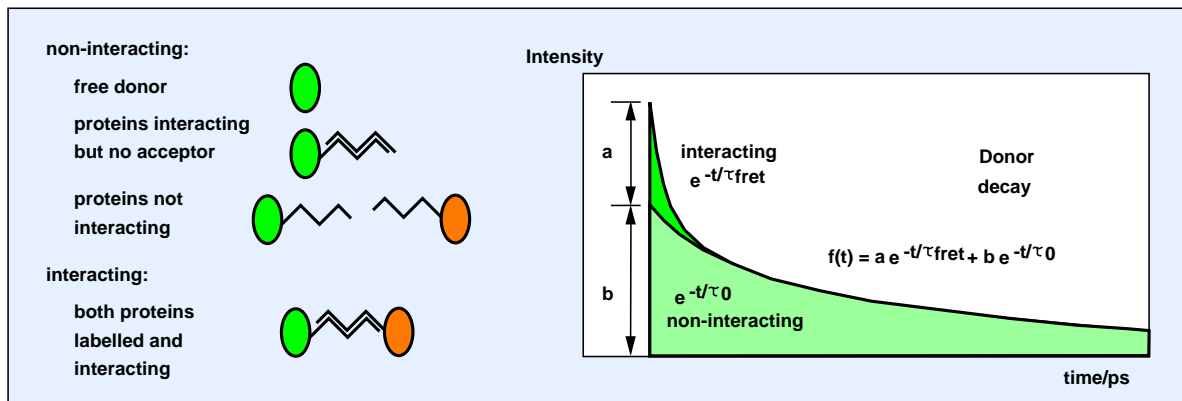


Fig. 56: Fluorescence decay components in FRET systems

Double exponential decay analysis delivers the lifetimes, τ_0 and τ_{FRET} , and the intensity factors, a and b , of the two decay components. From these parameters can be derived the true FRET efficiency, E_{fret} , the ratio of the distance and the Förster radius, r/r_0 , and the ratio of the number of interacting and non-interacting donor molecules, N_{fret} / N_0 :

$$E_{\text{fret}} = 1 - \tau_{\text{fret}} / \tau_0$$

$$(r/r_0)^6 = \tau_{\text{fret}} / (\tau_0 - \tau_{\text{fret}}) \quad \text{or} \quad (r/r_0)^6 = \frac{1}{E_{\text{fret}}} - 1$$

$$N_{\text{fret}} / N_0 = a / b$$

A typical decay curve of the donor fluorescence in a CFP-YFP system is shown in Fig. 57.

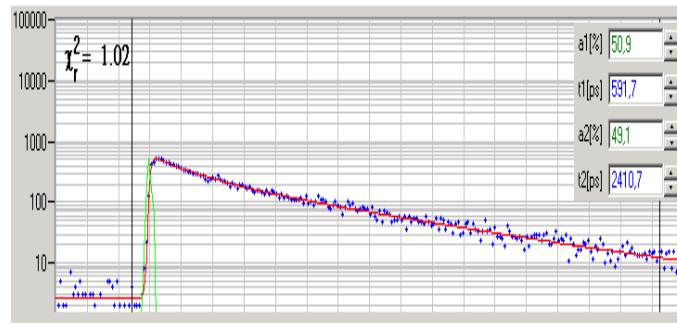


Fig. 57: Fluorescence decay curve measured in a CFP-YFP FRET system [15]. The decay profile is clearly double-exponential.

Similar double exponential decay behaviour is commonly found in FRET experiments based on multi-dimensional TCSPC [3, 11, 15, 16, 29, 35, 43, 84]. Double-exponential decay profiles have also been confirmed by streak-camera measurements [27, 28]. A summary of double-exponential FRET measurements is given in [18] and [19].

A general characterisation of TCSPC-FLIM FRET for monitoring protein interactions is given in [29, 38, 39, 84, 93]. Applications to protein interaction related to Alzheimer's disease are described in [3, 4, 21, 22, 23]. Interactions between the PCK and NK κ B signalling pathways have been investigated in [77]. FRET between GFP and RFP and FRET cascades from GFP via Cy3 into Cy5 are demonstrated in [85] and [1]. The agglutination of red blood cells by monoclonal antibodies was studied using FRET between Alexa 488 and DiI [90]. Interaction of the neuronal PDZ protein PSD-95 with the potassium channels and SHP-1-target interaction were studied in [27, 29]. It has also been shown that FRET can be used to monitor conformational changes of proteins in cells by FLIM-FRET [35, 74].

A detailed description of a TCSPC-FLIM-FRET system is given in [43]. The system is used for FRET between ECPF-EYFP and FM1-43 - FM4-64 in cultured neurones. FRET between ECFP and EYFP in plant cells was demonstrated in [31]. FRET measurements in plant cells are difficult because of the strong autofluorescence of the plant tissue. The authors show that two-photon excitation can be used to keep the autofluorescence signal at a tolerable level.

It has been attempted to obtain additional FRET information from the donor emission measured simultaneously with the donor emission in a dual-detector TCSPC system [59]. An a/b image of the acceptor decay should display the ratio of the acceptor emission excited via FRET and directly. The integral intensity of FRET-excited acceptor emission could then be used as a second way to obtain the net energy transfer rate. Unfortunately, in the CFP-YFP system, the acceptor decay cannot be observed directly because of the strong overlap of the donor fluorescence with the acceptor fluorescence spectrum. An attempt was made in [17] to subtract the donor bleedthrough from the acceptor decay and to build up an a/b image. In any case, using the acceptor fluorescence requires simultaneous detection of both the donor and acceptor images to reject photobleaching artefacts from the results.

A promising approach to the exploitation of the acceptor fluorescence is multi-wavelength FLIM [7, 14, 19, 30]. Reference spectra of the donor and the acceptor are recorded, and the FRET fluorescence is fit by a model containing these spectra and the unknown intensity coefficients and lifetimes of the donor and the acceptor. Thus, multi-wavelength FLIM may lead to a combination of FLIM-based and sensitised-emission FRET techniques. A demonstration of the technique has been given in [30].

Autofluorescence Microscopy of Tissue

Biological tissue contains a wide variety of endogenous fluorophores [69, 89]. However, the fluorescence spectra of endogenous chromophores are often broad, variable, and poorly defined. Moreover, the absorbers present in the tissue may change the apparent fluorescence spectra. It is therefore difficult to disentangle the fluorescence components by their emission spectra alone. Autofluorescence lifetime detection not only adds an additional separation parameter but also yields direct information about the metabolic state and the microenvironment of the fluorophores [72, 73, 81]. Moreover, autofluorescence imaging has benefits in cases when the reaction of tissue to optical radiation is to be investigated, such as tumor induction by UV irradiation. Such experiments forbid the use of exogenous fluorophores because energy or electron transfer from the fluorophores to the proteins could induce additional photodamage.

The samples used for tissue imaging are considerably thicker than samples containing single cells. Often tissue imaging is even performed on living animals. Therefore optical sectioning and a large penetration depth is required. The method of choice is therefore two-photon excitation with non-descanned detection.

The fluorescence decay profiles of tissue autofluorescence are multi-exponential, with decay components from about 100 ps to several ns. The deviations from single-exponential decay are substantial, see Fig. 58. Extracting meaningful decay parameters from the data therefore requires at least double-exponential analysis.

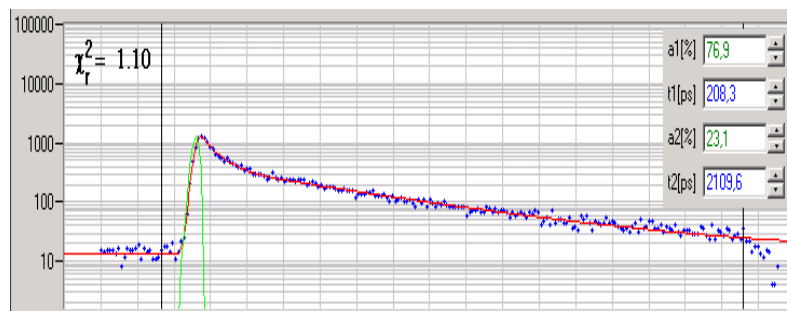


Fig. 58: Typical decay curve of tissue autofluorescence. Stratum corneum of human skin, two-photon excitation at 800 nm

The application of TCSPC FLIM to two-photon optical tomography of human skin was demonstrated in [17, 20, 68, 69, 70]. A summary is given in [18].

References

1. S.M. Ameer-Beg, N. Edme, M. Peter, P.R. Barber, T. Ng, B. Vojnovic, Imaging protein-protein interactions by multiphoton FLIM, *Proc. SPIE*, 5139, 180-189 (2003)
2. S.M. Ameer-Beg, P.R. Barber, R. Locke, R.J. Hodgkiss, B. Vojnovic, G.M. Tozer, J. Wilson, Application of multiphoton steady state and lifetime imaging to mapping of tumor vascular architecture in vivo, *Proc. SPIE*, 4620, 85-95 (2002)
3. B. J. Bacskai, J. Skoch, G.A. Hickey, R. Allen, B.T. Hyman, Fluorescence resonance energy transfer determinations using multiphoton fluorescence lifetime imaging microscopy to characterize amyloid-beta plaques, *J. Biomed. Opt* 8, 368-375 (2003)
4. B. J. Bacskai, J. Skoch, G.A. Hickey, O. Berezovska, B.T. Hyman, Multiphoton imaging in mouse models of Alzheimer's disease, *Proc. SPIE*, 5323, 71-76 (2004)
5. R.M. Ballew, J.N. Demas, An error analysis of the rapid lifetime determination method for the evaluation of single exponential decays, *Anal. Chem.* 61, 30 (1989)
6. Becker & Hickl GmbH, Routing modules for time-correlated single photon counting, manual, www.becker-hickl.com
7. Becker & Hickl GmbH, 16 channel detector head for time-correlated single photon counting, user handbook, available on www.becker-hickl.com, (2006)
8. Becker & Hickl GmbH, DCC-100 detector control module, manual, www.becker-hickl.com
9. Becker & Hickl GmbH, SPCImage Data Analysis Software for Fluorescence Lifetime Imaging Microscopy, www.becker-hickl.com
10. W. Becker, H. Hickl, C. Zander, K.H. Drexhage, M. Sauer, S. Siebert, J. Wolfrum, Time-resolved detection and identification of single analyte molecules in microcapillaries by time-correlated single photon counting, *Rev. Sci. Instrum.* 70, 1835-1841 (1999)
11. W. Becker, K. Benndorf, A. Bergmann, C. Biskup, K. König, U. Tirlapur, T. Zimmer, FRET measurements by TCSPC laser scanning microscopy, *Proc. SPIE* 4431, 94-98 (2001)
12. W. Becker, A. Bergmann, K. König, U. Tirlapur, Picosecond fluorescence lifetime microscopy by TCSPC imaging, *Proc. SPIE* 4262, 414-419 (2001)
13. W. Becker, A. Bergmann, H. Wabnitz, D. Grosenick, A. Liebert, High count rate multichannel TCSPC for optical tomography, *Proc. SPIE* 4431, 249-245 (2001)
14. W. Becker, A. Bergmann, C. Biskup, T. Zimmer, N. Klöcker, K. Benndorf, Multi-wavelength TCSPC lifetime imaging, *Proc. SPIE* 4620 79-84 (2002)
15. W. Becker, A. Bergmann, C. Biskup, L. Kelbauskas, T. Zimmer, N. Klöcker, K. Benndorf, High resolution TCSPC lifetime imaging, *Proc. SPIE* 4963, 175-184 (2003)
16. W. Becker, A. Bergmann, M.A. Hink, K. König, K. Benndorf, C. Biskup, Fluorescence lifetime imaging by time-correlated single photon counting, *Micr. Res. Techn.* 63, 58-66 (2004)
17. W. Becker, A. Bergmann, G. Biscotti, K. Koenig, I. Riemann, L. Kelbauskas, C. Biskup, High-speed FLIM data acquisition by time-correlated single photon counting, *Proc. SPIE* 5323, 27-35 (2004)
18. W. Becker, *Advanced time-correlated single-photon counting techniques*. Springer, Berlin, Heidelberg, New York, 2005
19. W. Becker, *The bh TCSPC handbook*. Becker & Hickl GmbH (2005), www.becker-hickl.com
20. W. Becker, A. Bergmann, E. Haustein, Z. Petrasek, P. Schwille, C. Biskup, L. Kelbauskas, K. Benndorf, N. Klöcker, T. Anhut, I. Riemann, K. König, Fluorescence lifetime images and correlation spectra obtained by multi-dimensional TCSPC, *Micr. Res. Techn.* 69, 186-195 (2006)

21. O. Berezovska, P. Ramdya, J. Skoch, M.S. Wolfe, B.J. Bacskai, B.T. Hyman, Amyloid precursor protein associates with a nicastrin-dependent docking site on the presenilin 1- γ -secretase complex in cells demonstrated by fluorescence lifetime imaging, *J. Neurosci.* 23, 4560-4566 (2003)
22. O. Berezovska, B.J. Bacskai, B.T. Hyman, Monitoring Proteins in Intact Cells, *Science of Aging Knowledge Environment*, SAGE KE 14 (2003)
23. O. Berezovska, A. Lleo, L.D. Herl, M.P. Frosch, E.A. Stern, B.J. Bacskai, B.T. Hyman, Familial Alzheimer's disease presenilin 1 mutations cause alterations in the conformation of presenilin and interactions with amyloid precursor protein, *J. Neurosci.* 25, 3009-3017 (2005)
24. K.M. Berland, P.T.C. So, E. Gratton, Two-photon fluorescence correlation spectroscopy, Method and application to the intracellular environment, *Biophys. J.* 68, 694-701 (1995)
25. T. Bernas, M. Zarebski, R.R. Cook, J.W. Dobrucki, Minimizing photobleaching during confocal microscopy of fluorescent probes bound to chromatin, role of anoxia and photon flux, *J. Microsc.* 215, 281-296 (2004)
26. D.K. Bird, K.W. Eliceiri, C-H. Fan, J.G. White, Simultaneous two-photon spectral and lifetime fluorescence microscopy, *Appl. Opt.* 43, 5173-5182 (2004)
27. C. Biskup, A. Böhmer, R. Pusch, L. Kelbauskas, A. Gorshkov, I. Majoul, J. Lindenau, K. Benndorf, F-D. Böhmer, Visualization of SHP-1-target interaction, *J. Cell Sci.* 117, 5155-5178 (2004)
28. C. Biskup, T. Zimmer, K. Benndorf, FRET between cardiac Na⁺ channel subunits measured with a confocal microscope and a streak camera, *Nature Biotechnology*, 22(2), 220-224 (2004)
29. C. Biskup, L. Kelbauskas, T. Zimmer, K. Benndorf, A. Bergmann, W. Becker, J.P. Ruppersberg, C. Stockklausner, N. Klöcker, Interaction of PSD-95 with potassium channels visualized by fluorescence lifetime-based resonance energy transfer imaging, *J. Biomed. Opt.* 9, 735-759 (2004)
30. C. Biskup, L. Kelbauskas, Th. Zimmer, S. Dietrich, K. Benndorf, W. Becker, A. Bergmann, N. Klöcker, Spectrally resolved fluorescence lifetime and FRET measurements, *Proc. SPIE* 5700, 188-196 (2005)
31. J.W. Borst, M.A. Hink, A. van Hoek, A.J.W.G. Visser, Multiphoton spectroscopy in living plant cells, *Proc. SPIE* 4963, 231-238 (2003)
32. S.Y. Breusegem, In vivo investigation of protein interactions in *C. Elegans* by Förster resonance energy transfer microscopy, University of Illinois at Urbana-Champaign (2002)
33. H. Brismar, B. Ulfhake, Fluorescence lifetime imaging measurements in confocal microscopy of neurons labeled with multiple fluorophores, *Nature Biotech.* 15, 373-377 (1997)
34. I. Bugiel, K. König, H. Wabnitz, Investigations of cells by fluorescence laser scanning microscopy with subnanosecond time resolution, *Lasers in the Life Sciences* 3(1), 47-53 (1989)
35. V. Calleja, S. Ameer-Beg, B. Vojnovic, R. Woscholski, J. Downwards, B. Larijani, Monitoring conformational changes of proteins in cells by fluorescence lifetime imaging microscopy, *Biochem. J.* 372, 33-40 (2003)
36. Y. Chen, J.D. Müller, P.T.C. So, E. Gratton, The Photon Counting Histogram in Fluorescence Fluctuation Spectroscopy, *Biophys. J.* 77, 553-567 (1999)
37. Y. Chen, J.D. Müller, Q.Q. Ruan, E. Gratton, Molecular brightness characterization of EGFP in vivo by fluorescence fluctuation spectroscopy, *Biophys. J.* 82, 133-144 (2002)
38. Y. Chen, A. Periasamy, Characterization of two-photon excitation fluorescence lifetime imaging microscopy for protein localization, *Microsc. Res. Tech.* 63, 72-80 (2004)

39. Y. Chen, A. Periasamy, Two-photon FIM-FRET microscopy for protein localization, *Proc. SPIE* 5323, 431-439 (2004)
40. W. Denk, J.H. Strickler, W.W.W. Webb, Two-photon laser scanning fluorescence microscopy, *Science* 248, 73-76 (1990)
41. Diaspro A. (ed.). *Confocal and two-photon microscopy: Foundations, applications and advances*. Wiley-Liss (2001)
42. P.S. Dittrich, P. Schwille, Photobleaching and stabilization of fluorophores used for single-molecule analysis with one- and two-photon excitation, *Appl. Phys. B* 73, 829-837 (2001)
43. R.R. Duncan, A. Bergmann, M.A. Cousin, D.K. Apps, M.J. Shipston, Multi-dimensional time-correlated single-photon counting (TCSPC) fluorescence lifetime imaging microscopy (FLIM) to detect FRET in cells, *J. Microsc.* 215, 1-12 (2004)
44. C. Eggeling, S. Berger, L. Brand, J.R. Fries, J. Schaffer, A. Volkmer, C.A. Seidel, Data registration and selective single-molecule analysis using multi-parameter fluorescence detection, *J. Biotechnol.* 86, 163 (2001)
45. K.W. Eliceiri, C.H. Fan, G.E. Lyons, J.G. White, Analysis of histology specimens using lifetime multiphoton microscopy, *J. Biomed. Opt.* 8, 376-380 (2003)
46. S. Felekyan, R. Kühnemuth, V. Kudryavtsev, C. Sandhagen, W. Becker, C.A.M. Seidel, Full correlation from picoseconds to seconds by time-resolved and time-correlated single photon detection, *Rev. Sci. Instrum.* 76, 083104 (2005)
47. Th. Förster, Zwischenmolekulare Energiewanderung und Fluoreszenz, *Ann. Phys. (Serie 6)* 2, 55-75 (1948)
48. C.D. Geddes, H. Cao, I. Gryczynski, J. Fang, J.R. Lakowicz, Metal-enhanced fluorescence (MEF) due to silver colloids on a planar surface: Potential applications of indocyanine green to in vivo imaging, *J. Phys. Chem. A* 107, 3443-3449 (2003)
49. H.C. Gerritsen, M.A.H. Asselbergs, A.V. Agronskaia, W.G.J.H.M. van Sark, Fluorescence lifetime imaging in scanning microscopes: acquisition speed, photon economy and lifetime resolution, *J. Microsc.* 206, 218-224 (2002)
50. M. Göppert-Mayer, Über Elementarakte mit zwei Quantensprüngen, *Ann. Phys.* 9, 273-294 (1931)
51. Govindjee, Sixty-three Years Since Kautsky: Chlorophyll α Fluorescence, *Aust. J. Plant Physiol.* 22, 131-160 (1995)
52. Govindjee, M.J. Seufferheld, Non-photochemical quenching of chlorophyll α Fluorescence: Early history and characterization of two xanthophyll-cycle mutants of *Chlamydomonas Reinhardtii*, *Funct. Plant Biol.* 29, 1141-1155 (2002)
53. A. Habenicht, J. Hjelm, E. Mukhtar, F. Bergström, L.B-A. Johansson, Two-photon excitation and time-resolved fluorescence: I. The proper response function for analysing single-photon counting experiments, *Chem. Phys. Lett.* 345, 367-375 (2002)
54. K.M. Hanson, M.J. Behne, N.P. Barry, T.M. Mauro, E. Gratton, Two-photon fluorescence imaging of the skin stratum corneum pH gradient, *Biophys. J.* 83, 1682-1690 (2002)
55. Hamamatsu Photonics K.K., R3809U-50 series Microchannel plate photomultiplier tube (MCP-PMTs) (2001)
56. Hamamatsu Photonics K.K., H7422 series Metal package PMT with cooler - photosensor modules (2003)
57. R.P. Haugland, *Handbook of fluorescent probes and research chemicals*, 7th Ed. Molecular Probes, Inc. (1999)
58. A. Hopt, E. Neher, Highly nonlinear Photodamage in two-photon fluorescence microscopy, *Biophys. J.* 80, 2029-2036 (2002)
59. M.K.Y. Hughes, S. Ameer-Beg, M. Peter, T. Ng, Use of acceptor fluorescence for determining FRET lifetimes, *Proc. SPIE* 5139, 88-96 (2003)

60. H. Kaneko, I. Putzier, S. Frings, U. B. Kaupp, and Th. Gensch, Chloride Accumulation in Mammalian Olfactory Sensory Neurons, *J. Neurosci.*, 24(36) 7931-7938 (2004)
61. L. Kelbauskas, W. Dietel, Internalization of aggregated photosensitizers by tumor cells: Subcellular time-resolved fluorescence spectroscopy on derivatives of pyropheophorbide-a ethers and chlorin e6 under femtosecond one- and two-photon excitation, *Photochem. Photobiol.* 76, 686-694 (2002)
62. J-P. Knemeyer, N. Marmé, M. Sauer, Probes for detection of specific DNA sequences at the single-molecule level, *Anal. Chem.* 72, 3717-3724 (2002)
63. M. Köllner, J. Wolfrum, How many photons are necessary for fluorescence-lifetime measurements?, *Phys. Chem. Lett.* 200, 199-204 (1992)
64. K. König, P.T.C. So, W.W. Mantulin, B.J. Tromberg, E. Gratton, Two-Photon excited lifetime imaging of autofluorescence in cells during UVA and NIR photostress, *J. Microsc.* 183, 197-204 (1996)
65. K. König, Multiphoton microscopy in life sciences, *J. Microsc.* 200, 83-104 (2000)
66. K. König, Laser tweezers and multiphoton microscopes on life science, *Histochem. Cell Biol.* 114, 79-92 (2000)
67. K. König, Cellular Response to Laser Radiation in Fluorescence Microscopes, in A. Periasamy, *Methods in Cellular Imaging*, Oxford University Press, 236-254 (2001)
68. K. König, U. Wollina, I. Riemann, C. Peuckert, K-J. Halbhuber, H. Konrad, P. Fischer, V. Fuenfstueck, T.W. Fischer, P. Elsner, Optical tomography of human skin with subcellular resolution and picosecond time resolution using intense near infrared femtosecond laser pulses, *Proc. SPIE* 4620, 191-202 (2002)
69. K. König, I. Riemann, High-resolution multiphoton tomography of human skin with subcellular spatial resolution and picosecond time resolution, *J. Biom. Opt.* 8, 432-439 (2003)
70. K. König, I. Riemann, G. Ehrlich, V. Ulrich, P. Fischer, Multiphoton FLIM and spectral imaging of cells and tissue, *Proc. SPIE* 5323, 240-251 (2004)
71. J.R. Lakowicz, I. Gryczynski, W. Wiczk, J. Kusba, M. Johnson, Correction for incomplete labeling in the measurement of distance distributions by frequency-domain fluorometry, *Anal. Biochem.* 195, 243-254 (1991)
72. J.R. Lakowicz, H. Szmajcinski, K. Nowaczyk, M.L. Johnson, Fluorescence lifetime imaging of free and protein-bound NADH, *PNAS* 89, 1271-1275 (1992)
73. J.R. Lakowicz, *Principles of Fluorescence Spectroscopy*, 2nd edn., Plenum Press, New York (1999)
74. A. Lleo, O. Berezovska, L. Herl, S. Raju, A. Deng, B.J. Bacskai, M.P. Frosch, M. Iriazary, B.T. Hyman, Nonsteroidal anti-inflammatory drugs lower A β 42 and change presenilin 1 conformation, *Nature Medicine* 10, 1065-1066 (2004)
75. J. Malicka, I. Gryczynski, C.D. Geddes, J.R. Lakowicz, Metal-enhanced emission from indocyanine green: a new approach to in vivo imaging, *J. Biomed. Opt.* 8, 472-478 (2003)
76. K. Maxwell, G.N. Johnson, Chlorophyll fluorescence - a practical guide, *Journal of Experimental Botany* 51, 659-668 (2000)
77. P.E. Morton, T.C. Ng, S.A. Roberts, B. Vojnovic, S.M. Ameer-Beg, Time resolved multiphoton imaging of the interaction between the PKC and NF κ B signalling pathways, *Proc. SPIE* 5139, 216-222 (2003)
78. J.D. Müller, Y. Chen, E. Gratton, Resolving Heterogeneity on the single molecular level with the photon-counting histogram, *Biophys. J.* 78, 474-586 (2000)
79. D.V. O'Connor, D. Phillips, *Time-correlated single photon counting*, Academic Press, London (1984)
80. G.H. Patterson, D.W. Piston, Photobleaching in two-photon excitation microscopy, *Biophys. J.* 78, 2159-2162 (2000)

81. R.J. Paul, H. Schneckenburger, Oxygen concentration and the oxidation-reduction state of yeast: Determination of free/bound NADH and flavins by time-resolved spectroscopy, *Naturwissenschaften* 83, 32-35 (1996)
82. J. Pawley (ed.), *Handbook of biological confocal microscopy*, 2nd edn., Plenum Press, New York (1995)
83. A. Periasamy, *Methods in Cellular Imaging*. Oxford University Press, Oxford New York (2001)
84. M. Peter, S.M. Ameer-Beg, Imaging molecular interactions by multiphoton FLIM, *Biology of the Cell* 96, 231-236 (2004)
85. M. Peter, S.M. Ameer-Beg, M.K.Y. Hughes, M.D. Keppler, S. Prag, M. Marsh, B. Vojnovic, T. Ng, Multiphoton-FLIM quantification of the EGFP-mRFP1 FRET pair for localization of membrane receptor-kinase interactions, *Biophys. J.* 88, 1224-1237 (2005)
86. M. Prummer, B. Sick, A. Renn, U.P. Wild, Multiparameter microscopy and spectroscopy for single-molecule analysis, *Anal. Chem.* 76, 1633-1640 (2004)
87. H. Qian, E.L. Elson, Distribution of molecular aggregation by analysis of fluctuation moments, *PNAS* 87, 5479-5483 (1990)
88. R. Rigler, E.S. Elson (eds), *Fluorescence Correlation Spectroscopy*, Springer Verlag Berlin, Heidelberg, New York (2001)
89. R. Richards-Kortum, R. Drezek, K. Sokolov, I. Pavlova, M. Follen, Survey of endogenous biological fluorophores. In M.-A. Mycek, B.W. Pogue (eds.), *Handbook of Biomedical Fluorescence*, Marcel Dekker Inc. New York, Basel, 237-264 (2003)
90. B. Riquelme, D. Dumas, J. Valverde, R. Rasia, J.F. Stoltz, Analysis of the 3D structure of agglutinated erythrocyte using CellScan and Confocal microscopy: Characterisation by FLIM-FRET, *Proc. SPIE* 5139, 190-198 (2003)
91. A. Rück, F. Dolp, C. Happ, R. Steiner, M. Beil, Time-resolved microspectrofluorometry and fluorescence lifetime imaging using ps pulsed laser diodes in laser scanning microscopes, *Proc. SPIE* 5139, 166-172 (2003)
92. R. Sanders, A. Draaijer, H.C. Gerritsen, P.M. Hout, Y.K. Levine, Quantitative pH Imaging in cells using confocal fluorescence lifetime imaging microscopy, *Analytical Biochemistry* 227, 302-308 (1995)
93. M. Snippe, J.W. Borst, R. Goldbach, R. Kormelik, The use of fluorescence microscopy to visualise homotypic interactions of tomato spotted wilt virus nucleocapsid protein in living cells, *J. Vir. Meth.* 125, 12-15 (2005)
94. P.T.C. So, K.H. Kim, L. Hsu, P. Kaplan, T. Haczewicz, C.Y. Dong, U. Greuter, N. Schlumpf, C. Buehler, Two-photon microscopy of tissues, in M.-A. Mycek, B.W. Pogue (eds.), *Handbook of Biomedical Fluorescence*, Marcel Dekker, New York, Basel, 181-208 (2003)
95. P. Theer, M.T. Hasan, W. Denk, Multi-photon imaging using a Ti:sapphire regenerative amplifier, *Proc. SPIE* 5139, 1-6 (2003)
96. P. Tinnefeld, V. Buschmann, D-P. Herten, K.T. Han, M. Sauer, Confocal fluorescence lifetime imaging microscopy (FLIM) at the single molecule level, *Single Mol.* 1, 215-223 (2000)
97. U.K. Tirlapur, K. König, Targeted transfection by femtosecond laser, *Nature* 418, 290-291 (2002)
98. B. Treanor, P.M.P. Lanigan, K. Suhling, T. Schreiber, I. Munro, M.A.A. Neil, D. Phillips, D.M. Davis, P.M.W. French, Imaging fluorescence lifetime heterogeneity applied to GFP-tagged MHC protein at an immunological synapse, *J. Microsc.* 217, 36-43 (2005)
99. M.A.M.J. Van Zandvoort, C.J. de Grauw, H.C. Gerritsen, J.L.V. Broers, M.G.A. Egbrink, F.C.S. Ramaekers, D.W. Slaaf, Discrimination of DNA and RNA in cells by a

- vital fluorescent probe: Lifetime imaging of SYTO13 in healthy and apoptotic cells, *Cytometry* 47, 226-232 (2002)
100. J.G. White, W.B. Amos, M. Fordham, An evaluation of confocal versus conventional imaging of biological structures by fluorescence light microscopy, *J. Cell Biol.* 105, 41-48 (1987)
101. J. Yguerabide, Nanosecond fluorescence spectroscopy of macromolecules, *Meth. Enzymol.* 26, 498-578 (1972)

Index

- Accumulate function 22
- Acquisition time 22, 35, 37
- ADC rate 34
- ADC resolution 22
- Aggregates 3
- Amplitudes of decay components 46
- Apparent lifetime 47
- Autofluorescence
 - lifetime 58
 - of tissue 58
- Autosave function 22
- Autoscale 24
- Beamsplitter assemblies 54
- Binning 44
 - pixels, during data acquisition 23
 - pixels, in lifetime analysis 44
- Block Info 28
- Blocking filters 14
- CFD parameters 22
- CFD rate 34
- Chi square 46, 47
- Clock signals, from scanner 7
- Collection time 22
- Complexes 2
- Components of decay function 46
- Confocal detection 9
- Count Rates 34
- Cycles, of a measurement 21
- D FLIM 8, 12
- Data analysis 39
- Data and Setup File Formats 27, 28
- DCC-100 11, 18
- Decay components 46
- Decay curve window 43
- Depth resolution, by two-photon excitation 9
- Detector control 18
- Detectors 11
 - beamsplitter assemblies 54
 - detector control 18
 - dual-detector systems 54
 - for confocal FLIM 53
 - for direct detection FLIM 52
 - for FCS 54
 - H7422P-40 53, 54
 - high efficiency 53
 - high resolution 52, 53
 - multi-spectral 53, 54
 - MW-FLIM detector 53, 54
 - PMC-100 11, 18, 52
 - R3809U 52, 53
- Diode laser 12
- Direct detection 10
- Display
 - autoscale 24
 - colours 25
 - display parameters 24
 - display scale 24
 - gated images 25
 - online display 24
- Efficiency of FLIM systems 4
- FCS 8, 21, 54
- File formats, data and setup 28
- File Formats, Data and Setup 27
- File Info 27, 28
- Files
 - block info 28
 - data and setup 27, 28
 - file info 27, 28
 - file name 27, 28
 - import into data analysis 41
 - loading of 28
 - saving of 27
 - standard setup files 29
- Fit procedure 39
- Fit selection parameters 43
- FLIM
 - acquisition time 37
 - autofluorescence of tissue 58
 - direct detection multiphoton 52
 - fluorescence quenching 55
 - FRET measurements 55
 - ion concentrations 55
 - multi-spectral 7, 53, 57
 - parameters 18
 - pH imaging 55
 - special system configurations 52
 - via RLD port 52
- FLIM measurement 31
- Fluorescence
 - decay functions 1, 3
 - fluorescence quenching 2
 - of complexes 2
 - quenching 55
 - resonance energy transfer 3
- Förster resonance energy transfer 55
- Frame size 14
- FRET 3, 55
 - acceptor emission 57
 - by multi-wavelength FLIM 57
 - double exponential 56
 - single exponential 56
- H7422P-40 53, 54
- Hardware Parameters 20, 23
- Histogram of lifetimes 50
- Image size 37
- Import, FLIM data into SPCImage 41
- Incomplete decay 46
- Instrument response function 39, 43
- Intensity image 42
- Ion concentrations 55
- IRF 39, 43, 50
- LCS software 14
- Life mode 22
- Lifetime images 39
 - autoscale of intensity 49
 - calculation of 39, 48
 - continuous colour 49
 - contrast and brightness 49
 - discrete colour 49
 - display 49
 - multi-exponential 40
 - parameter range 49
 - parameter to be displayed 49
 - time gating 49
- Lifetime, of autofluorescence 58
- Lifetimes of decay components 46
- Load 28
 - data files 28
 - file formats 28
 - files from older software versions 29

- load options 29
- predefined setups 30
- setup files 28
- Loading of FLIM data into SPCImage 41
- Lock 50
- Model function 46
- Model parameters 46, 48
- MP FLIM 8, 13
- MP laser 13
- Multi-spectral FLIM 53, 54
- Multi-wavelength FLIM 7, 57
- MW-FLIM detector 53, 54
- Nano particles 3
- Non-descanned detection 10
- Offset parameter 46
- One-photon excitation 8
- Online Display 24
- Operation mode 21
 - f(t,T) mode 21
 - FIFO mode 21
 - oscilloscope mode 21
 - scan sync in mode 21
 - scan sync out mode 21
 - single mode 21
 - steps and cycles 21
- Parameter constraints 46
- PCH 8, 21
- Photobleaching 35
- Photon counting histogram 8
- Pile-up effect 6
- Pinhole 9, 14
- Pixels, binning of 23
- Pixels, number of 22, 23
- PMC-100 52
- Polygone definition 50
- Predefined setups 30
- R3809U 52, 53
- Reference from Laser 11
- Region of interest 42
- Repeat function 22
- Repetition time 46
- Residuals 43
- RLD port 10, 52, 53
- Router 7, 54
- Routing windows 26
- Save 27
 - data files 27
 - file formats 27
 - setup files 27
- Scan
 - number of pixels 22
 - pixel number 14
 - scan clocks 11
 - scan parameters 23
 - scan rate 7
 - scan speed 14
 - scan windows 25
- Scatter parameter 46
- Selection of fit model 46
- Setup file names 30
- Setup for FLIM 12
- Shift parameter 46
- Shutter 11, 18
- Software, SPCM
 - display of images 24
 - display parameters 24
 - Loading of files 28
 - main panel 19
 - online display 24
 - predefined setups 30
 - saving files 27
 - system parameters 20
 - window parameters 25
- SPC-830 11
- SPCImage 39
- SPCM software 19
- Special commands 50
- Steps, of a measurement 21
- SYNC parameters 22
- SYNC rate 34
- System Configuration 11
- System Parameters 20, 23
- TAC parameters 22
- TAC rate 34
- TCSPC
 - classic TCSPC 5
 - detector signals 6
 - FIFO mode 8
 - multi-dimensional 6
 - multi-spectral 5
 - multi-wavelength 7
 - pile-up effect 6
 - router 7
 - time calibration 8
 - time channels 8
 - time resolution 8
 - time-tag mode 8
- Threshold for data analysis 44
- Time channels 22
- Time gating, of lifetime images 49
- Time windows 25
- Ti-Sapphire laser 13
- Trigger, of experiment 22
- Two-photon absorption 9
- Two-photon excitation 8, 9
- Unlock 50
- Window parameters 25
- X1 port 9, 11
- Zoom 37